Full title: Guanidine hydrochloride reactivates an ancient septin hetero-oligomer assembly pathway in budding yeast

Short title: Septin protein complex assembly and evolution

Courtney R. Johnson[1], Marc G. Steingesser[1], Andrew D. Weems[1], Anum Khan[2], Aurélie Bertin[3,4], Amy Gladfelter[2], and Michael A. McMurray[1,*]

[1]Department of Cell and Developmental Biology, University of Colorado Anschutz Medical Campus, Aurora, CO 80045 USA

[2]Department of Biology, University of North Carolina at Chapel Hill, Chapel Hill, NC 27599 USA

[3]Laboratoire Physico Chimie Curie, Institut Curie, PSL Research University, CNRS UMR 168, 75005, Paris, France.

[4]Sorbonne Université UPMC Univ Paris 06, 75005, Paris, France

*Corresponding author

E-mail: michael.mcmurray@cuanschutz.edu

ABSTRACT

Septin proteins co-assemble into hetero-oligomers that polymerize into cytoskeletal filaments with a variety of cellular functions. In *Saccharomyces cerevisiae*, where septins were first discovered, five subunits comprise two species of septin hetero-octamers, Cdc11/Shs1–Cdc12–Cdc3–Cdc10–Cdc10–Cdc3–Cdc12–Cdc11/Shs1. Septins evolved from ancestral GTPases. We previously found evidence that slow GTPase activity by Cdc12 directs the choice of incorporation of Cdc11 vs Shs1 into septin complexes. It was unclear why many septins, including Cdc3, lack GTPase activity. We serendipitously discovered that the small molecule guanidine hydrochloride (GdnHCl) rescues septin function in *cdc10* mutants by promoting assembly of non-native Cdc11/Shs1–Cdc12–Cdc3–Cdc3–Cdc12–Cdc11/Shs1 hexamers. We provide evidence that in *S. cerevisiae* Cdc3 guanidinium ion (Gdm) occupies the site of a “missing” Arg sidechain that is present in other fungal species in which (i) the Cdc3 subunit is an active GTPase and (ii) Cdc10-less hexamers co-exist with octamers in wild-type cells. These findings support a model in which Gdm reactivates a latent septin assembly pathway that was suppressed during fungal evolution in order to restrict assembly to hetero-octamers. Given recent reports that septin hexamers made natively in human cells also involve bypass of Cdc10-like central subunits via homodimerization of an active GTPase, our results provide new mechanistic details that likely apply to septin assembly throughout phylogeny.

AUTHOR SUMMARY

Life requires proper assembly of multi-subunit protein oligomers. The subunits of many oligomers evolved by gene duplication from a single ancestral protein. Specialization of inter-subunit interfaces ensures that subunit organization within these hetero-oligomers is non-random, but exactly how is often unclear. Hetero-oligomers of septin proteins perform a variety of cellular functions in nearly all eukaryotes. Subunit positioning within septin oligomers can often be predicted from sequence relatedness, yet the number and identity of subunits varies by organism and even within a single cell, raising the question of how the rules governing septin oligomer assembly can be simultaneously flexible and strict. We previously found that a septin's ability to hydrolyze the nucleotide GTP allows flexibility. Here we serendipitously discovered that a ten-atom molecule, guanidinium, appears to bind *in vivo* to a GTPase-dead septin where it promotes flexibility in oligomerization by mimicking the presence of an arginine sidechain found in active GTPases. Our findings suggest that loss of GTPase activity during evolution constrained septin oligomerization pathways. In addition to elucidating a mechanism that may be relevant to other oligomeric GTPases, the ability of guanidinium to rescue function *in vivo* of proteins lacking specific arginines has both evolutionary and therapeutic implications.

INTRODUCTION

Septin proteins are found in nearly every eukaryotic lineage, with the exception of land plants (1–4). In most extant organisms studied to date, multiple septin proteins co-assemble into linear, rod-shaped hetero-oligomers with at least some potential to polymerize into filaments (5–7). Septin hetero-oligomers are now known to contribute functionally to a wide variety of cellular processes (8,9). A number of human diseases and disorders, ranging from cancer to male infertility, have been linked to septin dysregulation or mutation (8,9), but within our understanding of septin roles in cellular function one common theme emerges: the ability to assemble into quaternary complexes is key.

All distinct septins share clear homology, but phylogenetic analysis reveals septin groups and subgroups (3) that can accurately predict which septin occupies which subunit position within hetero-oligomers (10). However, the subtleties of the distinctions between septins that drive assembly of hetero-oligomers with precise subunit organization remain incompletely understood. Moreover, the oligomerization interfaces have clearly not diverged drastically from the ancestral form, as nearly all septins retain the ability to robustly homo-oligomerize *in vitro* (11,12) whether or not they do so *in vivo*. How cells assemble specific septin hetero-oligomers to meet functional demands represents a major focus of septin research. More generally, septins provide a powerful model to study the mechanisms by which multisubunit complexes are assembled with high efficiency and fidelity in living cells.

Septins clearly evolved from an ancestral GTPase (13) but multiple septins subsequently lost the ability to hydrolyze GTP. Unlike the building blocks of polymers of the other cytoskeletal NTPases actin and tubulin (and their prokaryotic counterparts), in native septin hetero-oligomers most, if not all, of the septin nucleotide-binding pockets are buried within an oligomerization interface, called the G interface (14). Particularly for septin complexes in budding yeast, where hetero-octamers polymerize into filaments via the other, so-called “NC” septin-septin interface (14,15), burial of GTP in G interfaces within highly stable complexes severely limits the potential for cycles of GTP binding, hydrolysis, and exchange to modulate the assembly and disassembly of septin filaments. Nonetheless, most septins retain sequences clearly corresponding to regions/motifs in other small GTPases that contact bound nucleotide and/or change conformation upon GTP hydrolysis. These include the G1/Walker/P-loop, residues of which contact each of the three phosphates; the G2/Switch I and G3/Switch II loops, which are in proximity to the γ phosphate when it is present but are in distinct locations when it is absent; and the G4 motif, which contacts the base and dictates specificity for guanosine nucleotides. The question of what roles GTP binding and hydrolysis play

in septin biogenesis and function has been a major focus in septin research for over two decades (16).

The baker's yeast, *Saccharomyces cerevisiae*, has been at the forefront of septin research, for a number of reasons. The repertoire of septin proteins expressed in yeast (seven) is much simpler than that of humans (thirteen). Two yeast septins are expressed and function specifically during the process of sporulation (17–21), a version of gametogenesis, leaving five septins expressed in nearly stoichiometric amounts (22) in mitotically dividing cells: Cdc3, Cdc10, Cdc11, Cdc12, and Shs1. Yeast septin localization during the mitotic cell division cycle is primarily restricted to the cortex, where the septins take the form of filamentous rings at the mother-bud neck that undergo a series of discrete structural transitions as the bud emerges and grows and cytokinesis and cell separation take place (6). Septin filament assembly is essential for proliferation (23), and septin ring assembly, bud morphogenesis and cytokinesis are grossly perturbed in viable septin mutants (24), providing clear readouts for defects in septin biogenesis (25). A combination of molecular genetic (11,23,26–28), biochemical (11,12,15,28), and structural (12,14,15,28) approaches have demonstrated that two kinds of hetero-octamers co-exist, with a linear hexameric core of the order Cdc12–Cdc3–Cdc10–Cdc10–Cdc3–Cdc12 "capped" at each end with either Cdc11 or Shs1. While the functional basis for yeast octamer diversity remains largely unknown, at the level of quaternary structure septins are best understood in *S. cerevisiae*.

We are most interested in the mechanisms of assembly of septin hetero-oligomers, and previously used mutants isolated in unbiased genetic screens to elucidate roles in this process for nucleotide binding (29) and interactions with cytosolic chaperones (30), including the fungal disaggregase Hsp104, a hexameric AAA+ ATPase (31). Here we report that the function of specific septin mutants is affected in unexpected ways by guanidine hydrochloride (GdnHCl), a small molecule used for decades to inhibit Hsp104 ATPase activity *in vivo* (32,33). Our findings reveal important roles for

114 specific residues and structural motifs in septin hetero-oligomer assembly, suggest a series of key
115 events during fungal septin evolution that enforced incorporation of Cdc10 subunits in hetero-
116 oligomers, and provide what is, to our knowledge, the first evidence that guanidinium (Gdm) has the
117 potential to functionally replace Arg residues *in vivo*.
118
119 RESULTS
120 **GdnHCl restores high-temperature septin function to *cdc10* mutants in an Hsp104-**
121 **independent manner**
122 We previously reported interactions between an ATPase-dead mutant of Hsp104 and a
123 temperature-sensitive (TS) mutant of Cdc10, in which overexpression of the mutant Hsp104
124 inhibited the proliferation of *cdc10(D182N)* cells at an otherwise permissive low temperature (27ºC)
125 (30). We expected that the addition of 3 mM GdnHCl to the culture medium would mimic these
126 inhibitory effects in cells with wild-type (WT) Hsp104. Instead, we found complete rescue by GdnHCl
127 of the *cdc10(D182N)* TS proliferation defect at all temperatures tested (up to 37ºC) (Fig 1A). GdnHCl
128 did not have the same effect on cells carrying TS alleles of other septins, although in its presence
129 a *cdc12(G247E)* strain grew slightly worse at 30ºC and slightly better at 37ºC (Fig 1A). To our
130 surprise, GdnHCl rescue of *cdc10(D182N)* did not require Hsp104 (Fig 1B). Others have suggested
131 that a mitochondrial Hsp104 homolog, Hsp78, might share functions with Hsp104 (34), and Hsp78
132 and Hsp104 share the same residues within the ATP binding pocket that contact Gdm in the
133 bacterial Hsp104 homolog ClpB (Fig 1C), but Hsp78 was also dispensable for GdnHCl rescue of
134 *cdc10(D182N)* high-temperature growth (Fig 1B). Inhibition of Hsp104 (i.e., curing of prions) or
135 Hsp78 (i.e., induction of cytoplasmic petites) by GdnHCl *in vivo* requires concentrations in the
136 medium of ≥1 mM (35), but GdnHCl was sufficient to provide partial rescue of 37ºC growth by
137 *cdc10(D182N)* cells at concentrations <0.1 mM (Fig 1D,E). We conclude that GdnHCl suppresses
138 septin defects in *cdc10(D182N)* mutants via a mechanism that does not involve Hsp104 or its

139 homolog Hsp78.

140

141 **GdnHCl drives exclusion of mutant Cdc10 molecules from higher-order septin structures**

142 We previously noted that the *cdc12(G247E)* mutation appears to decrease the levels of WT Cdc10
143 (30). Cells tolerate loss of Cdc10 by assembling filaments via hexameric building blocks in which
144 Cdc3 forms a non-native G homodimer, but *cdc10Δ* cells are TS due to thermal instability of the
145 non-native Cdc3 homodimer (23). Rescue of the TS defects at 37ºC of the *cdc10(D182N)* and
146 *cdc12(G247E)* mutants by GdnHCl could reflect stabilization of Cdc10-less hexamers, rather than
147 any specific effect on the *cdc10(D182N)* allele. Consistent with this idea, GdnHCl also fully
148 suppressed the TS phenotype resulting from *cdc10(G100E)* mutation (S1 Fig), as well as that of
149 *cdc10Δ* (Fig 2A). Clear but partial GdnHCl rescue was also observed for *cdc10(G44D)* cells (S1
150 Fig). We confirmed via immunofluorescence with anti-Cdc11 antibodies (S1 Fig) and electron
151 microscopy (S1 Fig) that at 37ºC GdnHCl-treated *cdc10* cells assembled filamentous rings
152 composed of other septins. Thus GdnHCl does not simply bypass the need for septin filaments.

153

154 Given these results, we wondered if in cells carrying point-mutant *cdc10* alleles GdnHCl bypasses
155 altogether the incorporation of the mutant Cdc10 subunits during septin hetero-oligomer assembly.
156 Indeed, even at temperatures permissive in the absence of GdnHCl for septin ring incorporation of
157 Cdc10(D182N)-GFP, in the presence of 3 mM GdnHCl the fluorescence of Cdc10(D182N)-GFP
158 was restricted to the cytoplasm (Fig 2B). WT Cdc10-GFP, on the other hand, continued to localize
159 to the bud neck despite the presence of GdnHCl (Fig 2B). Similarly, in diploid cells co-expressing
160 Cdc10-mCherry and Cdc10(D182N)-GFP, the addition of GdnHCl specifically eliminated
161 Cdc10(D182N) incorporation in septin rings, with no obvious effect on WT Cdc10 (Fig 2C). Our
162 results suggest that when mutations within the Cdc10 G interface perturb the ability of Cdc10 to

163 acquire a conformation that binds tightly to Cdc3, GdnHCl allows other Cdc3 molecules to
164 outcompete the mutant Cdc10 proteins for occupancy of the Cdc3 G interface, ultimately co-
165 assembling with Cdc11, Cdc12, and Shs1 into Cdc10-less hexamers capable of robust septin
166 functions. As predicted from this model, GdnHCl was unable to rescue *cdc10Δ* growth when Cdc3
167 carried a mutation (W364A) previously shown (23) to block Cdc3 homodimerization (Fig 2D).
168

169 **GdnHCl promotes Cdc10-less filament assembly *in vitro* from purified, recombinant**
170 **complexes**

171 Yeast septin function is regulated (in poorly defined ways) by a large number of pathways (36),
172 which could be altered by GdnHCl to indirectly promote Cdc3 homodimerization. To ask if GdnHCl
173 is able to promote Cdc10-less septin filament assembly outside of yeast cells, we co-expressed
174 Cdc3, Cdc11, and hexahistidine-tagged Cdc12 (6xHis-Cdc12) in *E. coli*, which normally lacks
175 septins, and purified trimeric Cdc3–6xHis-Cdc12–Cdc11 complexes using high-salt buffers, as
176 described previously (12,15,23). We then used centrifugal sedimentation of septin filaments
177 followed by densitometry of Coomassie-stained bands on SDS-PAGE gels (Fig 3) to ask if these
178 complexes could form hexamers and polymerize into filaments *in vitro* upon salt dilution. We
179 observed some truncation of the C terminus of Cdc11 during expression/purification, as well as co-
180 purification of the *E. coli* chaperonin GroEL, which binds indiscriminately to affinity beads (37) and
181 co-migrates with Cdc3 (Fig 3). Hence we paid most attention to the amounts of 6xHis-Cdc12.
182

183 Previous studies found that ~35% of Cdc10-less complexes sediment in these conditions, compared
184 to ~80% of Cdc10-containing octamers (12), consistent with poor hexamer (and thus filament)
185 formation in the absence of Cdc10. We found similar results (Fig 3). To test effects of GdnHCl, we
186 either grew the bacteria in the presence of 100 mM GdnHCl and kept GdnHCl in all buffers
187 thereafter, or we only introduced the GdnHCl during polymerization. The presence of GdnHCl during

188 expression, purification, and polymerization was associated with an increase in septin complex
189 sedimentation (Fig 3). Adding GdnHCl just prior to polymerization had a subtler effect (Fig 3). 100
190 mM is well below GdnHCl concentrations that begin to unfold globular proteins (38), and the other
191 septins remained stoichiometrically associated with 6xHis-Cdc12 in the presence of 100 mM
192 GdnHCl (Fig 3), which we take as evidence that sedimentation reflected authentic filament
193 polymerization, rather than GdnHCl-induced partial denaturation and subsequent non-specific
194 aggregation. We conclude from these data that GdnHCl is able to promote septin filament assembly
195 by recombinant Cdc10-less septin complexes produced in a heterologous system that lacks septin-
196 regulatory pathways. Thus GdnHCl likely acts directly on septin proteins, and seems to work best
197 when present during septin folding/assembly.
198

199 **Unbiased *in silico* modeling and phylogenetic analysis point to Thr302 as the site of Gdm**
200 **binding in Cdc3**

201 Using an unbiased genetic approach, we previously identified a spontaneous mutation in the Cdc3
202 G interface, G261V, that improves the proliferation of *cdc10*Δ cells, and concluded that the
203 introduction of Val in this position stabilizes a conformation of the G interface that is more competent
204 for self-association than the major conformation populated by WT Cdc3 at high termperatures (23).
205 We reasoned that Gdm might bind in the Cdc3 G interface and similarly promote the
206 homodimerization-competent conformation. For clues as to where Gdm might bind, we first used
207 the structure of human SEPT2 bound to the non-hydrolyzable nucleotide analog 5'-guanylyl
208 imidodiphosphate (GppNHp) (39) to generate a homology model of the globular domain of
209 monomeric Cdc3, and then performed unbiased *in silico* docking simulations to ask for the lowest-
210 energy predicted sites of Gdm binding. Four sites had binding free energies of ≤-3 kcal/mol. One
211 site, between the sidechains of Thr302 and His262, lies in the G interface, and had the second-
212 lowest predicted free energy of binding (Fig 4A).
213

214 As a parallel approach, we considered that (i) Gdm mimics the distal end of an Arg sidechain, and
215 (ii) a number of previous *in vitro* studies of diverse non-septin proteins – including T4 lysozyme (40),
216 β-galactosidase (41), and carboxypeptidase A (42) – demonstrated that Gdm is able to functionally
217 occupy molecular vacancies that are created by the replacement of an Arg residue with residues
218 having smaller sidechains (e.g. Ala). We thus hypothesized that one or more Arg residues might
219 contribute to G interface contacts for other septins that are, unlike *S. cerevisiae* Cdc3, capable of
220 robust G homodimerization.
221
222 To identify candidate Arg residues, we performed a phylogenetic analysis of Cdc3 homologs from
223 different species, which we separated into two categories based on the severity of phenotypes
224 accompanying deletion of the *CDC10* homolog. If non-*Saccharomyces* species possess an Arg that
225 favors G homodimerization by Cdc3, then we predicted this group of species should easily form
226 Cdc10-less septin hexamers and be better able to tolerate deletion of the Cdc10 homolog. Such
227 functional information is available for non-*Saccharomyces* species from eleven distinct fungal
228 genera. In *Aspergillus* (*fumigatis* (43) or *nidulans* (44)), *Candida albicans* (45), *Cryptococcus*
229 *neoformans* (46), *Fusarium graminearum* (47), *Neurospora crassa* (48), *Schizosaccharomyces*
230 *pombe* (49), and *Ustilago maydis* (50), deletion of the Cdc10 homolog has distinctly milder
231 phenotypic consequences compared to deletion of the Cdc3 homolog. In *Magnaporthe oryzae*,
232 septin ring assembly is perturbed by deletion of any septin, but higher-order, filamentous structures
233 persist in cells lacking the Cdc10 homolog Sep4, whereas in the other mutants septin localization
234 is almost exclusively diffuse (51). Finally, in *Coprinopsis cinerea*, a UV-induced mutant defective in
235 fruiting body development was rescued by a gene encoding CcCdc3, but the expression of CcCdc10
236 remained about 100-fold decreased in the mutant following rescue, suggesting that the mutant was
237 defective in both CcCdc3 and CcCdc10 expression, and that rescue of CcCdc3 expression was
238 sufficient to restore function (52). We interpret these results as evidence that in *C. cinerea*, as well,
239 loss of Cdc10 is better tolerated than loss of Cdc3.

240

241 By contrast, only the Shs1 homolog is non-essential for proliferation in *Kluyveromyces lactis* (53).
242 In *Ashbya gossypii*, deletion of any mitotic septin prevents septin ring assembly; loss of the Cdc10
243 homolog is as severe as loss of the Cdc3 homolog (54). According to our hypothesis, if there is a
244 key Arg residue that promotes Cdc3 homodimerization, and *S. cerevisiae* lacks it, then *K. lactis* and
245 *A. gossypii* should also lack it.

246

247 S2 Fig shows an alignment of protein sequences for Cdc3 homologs from the fungal species listed
248 above. As ScCdc3 is predicted to be unable to hydrolyze GTP (39), we also included for comparison
249 human SEPT2 and SEPT9, because for these septins crystal structures are available of non-native
250 G homodimers in the "GTP state" (bound to the non-hydrolyzable GTP analogs GppNHp or GTPγS,
251 respectively). Only sixteen residues were distinctly different between a group including *S. cerevisiae*
252 and the two species that cannot tolerate Cdc10 loss, and the group of species that tolerate *CDC10*
253 deletion. For six of these residues, the changes reflect substitutions with strong predicted effects on
254 amino acid properties (polarity, charge, size, etc.). One of these non-conservative variants lies in
255 the C-terminal extension, which is disordered in septin crystal structures. Based on the crystal
256 structures of SEPT2•GppNHp and SEPT9•GTPγS, all of the other five non-conservative variants
257 cluster near the G interface (Fig 4B), and one of these residues – corresponding to Thr302 in
258 ScCdc3 – is an Arg in eight of the nine species that tolerate Cdc10 loss (S2 Fig). Moreover, in the
259 SEPT2•GppNHp structure the Gdm group of the corresponding Arg in SEPT2 is located in the same
260 place where our *in silico* docking results predicted that Gdm binds to Cdc3, between Thr302 and
261 His262 (Fig 4). Together, these findings strongly support the idea that Gdm promotes Cdc3
262 homodimerization by occupying the same site in the Cdc3 G interface that in other septins is
263 occupied by the Gdm moiety of an Arg sidechain. This Arg residue was likely substituted to Thr
264 during the evolution of the fungal lineage that includes *S. cerevisiae*, *A. gossypii*, and *K. lactis*,
265 concomitant with loss of Cdc10-less hexamers in these yeasts.

266

267 **GdnHCl promotes higher-order septin assembly in *A. gossypii* cells lacking Cdc10**

268 Our phylogenetic comparisons predicted that Gdm should act similarly on the *A. gossypii* Cdc3
269 homolog to promote AgCdc3 homodimerization in the absence of Cdc10. To test this prediction, we
270 exposed *A. gossypii* cells lacking *CDC10* to GdnHCl and assessed higher-order septin assembly
271 by monitoring the localization of Shs1-GFP expressed in the same cells. As reported previously
272 (54), in the absence of GdnHCl Shs1-GFP fluorescence was cytoplasmic and diffuse (Fig 5).
273 Addition of GdnHCl restored the localization of Shs1-GFP to branch points and hyphal tips (Fig 5),
274 the same pattern observed in WT cells (54). Thus the ability of GdnHCl to promote septin function
275 in the absence of Cdc10, and the loss of Arg at the position corresponding to ScCdc3 Thr302, are
276 both conserved over >100m years of evolution.

277

278 **Chemical rescue of *cdc10* by Gdm derivatives**

279 To better understand the molecular details of Gdm "rescue" of Arg-substituted mutants, earlier *in*
280 *vitro* Gdm studies also tested other small molecules with similar chemical properties, including urea
281 and the GdnHCl derivatives aminoguanidine (Pimagedine, here "aGdnHCl") and N-ethylguanidine
282 ("eGdnHCl") (55). We undertook an analogous approach to study GdnHCl rescue of the *cdc10* TS
283 phenotype.

284

285 First, we tested urea, which differs from Gdm by only a few atoms (Fig 6A). We grew WT or *cdc10*
286 cells on solid rich medium containing 0.64 M urea, a concentration we found to slow, but not prevent,
287 growth of WT cells, and saw no *cdc10* rescue (Fig 6A-B). To test a gradient of concentrations, we
288 also placed filter disks soaked with GdnHCl or urea on lawns of WT or *cdc10* cells. We saw a clear
289 zone of rescue around the GdnHCl disk, but not with urea (Fig 6C). We next exposed WT or *cdc10*
290 cells to 0.375 mM GdnHCl, aGdnHCl, eGdnHCl, or combinations of GdnHCl plus eGdnHCl or
291 GdnHCl plus aGdnHCl (0.375 mM each). At 0.375 mM GdnHCl provided only a partial rescue (Fig

292 6D), allowing us to detect subtle effects of the GdnHCl derivatives when combined with GdnHCl. At
293 22ºC, 0.375 mM of any single drug had no noticeable effect on growth; slight growth inhibition of
294 both WT and mutant cells was observed when the total concentration of GdnHCl plus derivative
295 was 0.75 mM (Fig 6D). At 37ºC, in addition to the expected partial *cdc10* rescue by GdnHCl, there
296 was a very slight rescue by eGdnHCl, and an even less pronounced rescue by aGdnHCl (Fig 6D).
297 By contrast, mixing GdnHCl with aGdnHCl or eGdnHCl to a total concentration of 0.75 mM resulted
298 in full or nearly full rescue of *cdc10* 37ºC growth, respectively (Fig 6D). We interpret these findings
299 to mean that aGdm and eGdm (the guanidinium ion derivatives) occupy the position between Cdc3
300 Thr302 and His262 differently than does Gdm. They may not provide the appropriate molecular
301 contacts across the G dimer interface, or they may bind less well, or even too well (if Gdm acts only
302 transiently during Cdc3 folding). Indeed, aGdm and eGdm were predicted by *in silico* modeling to
303 bind in the same location as Gdm but with lower free energies, with the additional moieties projecting
304 in various directions (Fig 6E) in ways that might further alter Cdc3 conformation. It is also possible
305 that yeast cells are less permeable to these GdnHCl derivatives. Urea does not rescue at all,
306 possibly because it cannot form a cation. Finally, as would be expected if only small molecules like
307 Gdm can fit into the pocket provided by Thr302 and surrounding residues, 5 mM arginine
308 hydrochloride in the medium provided no *cdc10* rescue (Fig 6F).
309

310 **Mutating Cdc3 Thr302 to Arg prevents *cdc10*Δ rescue by GdnHCl**

311 To test if the absence of Arg at ScCdc3 position 302 is sufficient to explain the inability of *S.*
312 *cerevisiae cdc10*Δ cells to proliferate at 37ºC, we replaced Thr302 with Arg. The double-mutant
313 *cdc10*Δ *cdc3(T302R)* cells were, like *cdc10*Δ *CDC3*$^+$, temperature-sensitive, but unlike *cdc10*Δ
314 *CDC3*$^+$ the addition of GdnHCl failed to restore proliferation at 37ºC (Fig 7). By contrast, when we
315 replaced Thr302 with an amino acid with similar properties, Val, we saw rescue by Gdm (Fig 7). We
316 interpret these data as evidence that Gdm binds to ScCdc3 near Thr302 (or Val302) in order to
317 promote homodimerization, but does so in a way that is not recapitulated by an Arg sidechain.

318 Instead, Arg302 blocks functional Gdm binding. We conclude that the T302R substitution alone
319 cannot "reverse evolution", yet GdnHCl does. How?
320

321 **Arg or Gdm at ScCdc3 position 302 likely "tunes" a key His residue within the G homodimer**
322 **interface**

323 ScCdc3 Thr302 is predicted to lie within the septin α4 helix, which is located near both the nucleotide
324 binding pocket and the G interface (Fig 4). To begin to understand the molecular mechanism by
325 which Gdm at this position promotes Cdc3 homodimerization, we first examined thirteen available
326 septin crystal structures and asked which other residues are nearby the residue in the position
327 equivalent to Thr302. The only non-α4-helix residue within 5 Å in every structure was a highly
328 conserved His (Table 1) residing in a loop at the end of the β4 strand previously dubbed the "*trans*
329 loop 1" (56), the same His predicted by our *in silico* modeling to contact bound Gdm in Cdc3 (Fig
330 4A). In SEPT2•GppNHp, His158 contacts a highly conserved Asp within the Switch II loop of the
331 other protomer (Fig 4B) (39). By contrast, in the sole *Chlamydomonas reinhardtii* septin, CrSEPT,
332 (57) or in human SEPT9•GTPγS, the *trans* loop 1 His instead contacts the nucleotide bound by the
333 other protomer (Fig 4B). Thus, depending on which septins are involved, this key His residue makes
334 either of two distinct contacts across the septin G dimer interface. If during hetero-oligomerization
335 two alternative septins (e.g. Cdc3 or a mutant Cdc10) present to Cdc3 "competing" G interfaces in
336 distinct conformations, then the position of the *trans* loop 1 His may dictate which is ultimately
337 chosen for incorporation, and Gdm could influence this choice.

Table 1. Residues in close proximity to the positions corresponding to ScCdc3 Thr302 or His262 for other septins with solved crystal structures.

PDB entry, Septin•nucleotide (oligomeric state)	***Residues within 5Å (capitalized) of position corresponding to ScCdc3 Thr302****	***Residues within 5Å (capitalized) of His corresponding to ScCdc3 His262***
2QNR, HsSEPT2•GDP (G dimer)	*trans* loop 1 (pfg**H**Glkp)	α4 (reRLkk**R**ildE)
2QA5, HsSEPT2•GDP (G dimer)	*trans* loop 1 (pfg**H**glkp)	α4 (rerLkk**R**ilde)
3FTQ, HsSEPT2•GppNHp (G dimer)	*trans* loop 1 (pfg**H**Glkp)	α4 (rerLkk**R**ildE), Switch I (kieRtvq)**, Switch II (dtpgygDain)**
4Z51, HsSEPT3•GppNHp (monomer)	*trans* loop 1 (ptG**H**Slrp)	α4 (kseFkq**R**vrkE)
3SOP, HsSEPT3•GDP (G dimer)	*trans* loop 1 (ptG**H**Slrp)	α4 (kseFkq**R**vrke), P-loop (gqSGlgk)**, Switch I (vIPKtve)**
4Z54, HsSEPT3•GDP (G dimer)	*trans* loop 1 (ptG**H**Slrp)	α4 (kseFkq**R**vrkE), P-loop (gqSGlgk)**, Switch I (eeKIPKtve)**
3T5D, HsSEPT7•GDP (G dimer)	*trans* loop 1 (psg**H**Glkp)	α4 (qqFkk**Q**im), P-loop (geSGlgk)**
3TW4, HsSEPT7•GDP (G dimer)	*trans* loop 1 (psg**H**GLkp)	α4 (qqFkk**Q**im), P-loop (geSGlgk)**
5CYO, HsSEPT9•GDP (G dimer)	*trans* loop 1 (atG**H**Slrp)	α4 (rvhFkq**R**Itad), P-loop (gqSGlgk)**, Switch I (eeRIPKtie)**
5CYP, HsSEPT9•GTPγS (G dimer)	*trans* loop 1 (atg**H**SLrp)	α4 (rvhFkq**R**Itad), P-loop (gqsGlgk)**, Switch I (eeRIPKtie)**
4KV9, SmSEPT10•GDP (G dimer)	*trans* loop 1 (ptG**H**Slks)	α4 (lqkFka**R**ilse), P-loop (geTGigk)**
4KVA, SmSEPT10•GTP (G dimer)	*trans* loop 1 (ptG**H**Slks)	α4 (lqkFka**R**ilse), P-loop (geTgigk)**
5AR1, ScCdc11•empty (quasi-G dimer)***	*trans* loop 1 (ptg**H**Glke)	α4 (lklnkk**L**imeD)

* Residues at positions corresponding to ScCdc3 Thr302 were identified based on structure-guided alignments. SEPT2, Arg198; SEPT3, Arg224; SEPT7, Gln210; SEPT9, Arg442; SEPT10, Arg199; Cdc11, Leu187.
** Residues from the other protomer across the G interface.
***Dimer in solution is mediated by the C-terminal extension, and is unaffected by G interface mutations, thus contacts across the G interface are presumably crystal-induced.

338

339 In SEPT2•GppNHp, His158 is positioned in *cis* by contacts (~3 Å) with a Glu residue (Glu202) (39),

340 which lies one turn away from Arg198 in the α4 helix (Fig 4B). The Gdm moeity of SEPT2 Arg198

341 (residue corresponding to Thr302 in Cdc3) is also within ~3 Å of the backbone amide carbonyl of

342 His158 (Fig 4B, Table 1), and thus is equally well located to position His158. In CrSEPT and
343 SEPT9•GTPγS, the Arg198 equivalent instead contacts the Glu202 equivalent (Fig 4B). Thus in
344 some but not all septins the Gdm moiety of the α4 Arg is ideally positioned to contact the *trans* loop
345 1 His and thereby potentially bias partner choice during septin G dimerization. By contacting His262,
346 Gdm bound near Thr302 in Cdc3 could bias Cdc3 towards homodimerization and away from
347 heterodimerization with Cdc10.
348
349 To look for additional evidence in support of this model, we next asked which other residues are
350 located in the vicinity (≤5 Å) of the *trans* loop 1 His in thirteen available septin crystal structures. The
351 α4 helix was the only region to meet this criterion in every structure, and, as expected, when Arg
352 was present at the position corresponding to ScCdc3 Thr302, it was always within 5 Å (Table 1).
353 Apart from the α4 helix, the Switch II loop, and adjacent *trans* loop 1 residues, residues within 5 Å
354 of the His fell within only two other regions: the P-loop and the Switch I loop (Table 1). Remarkably,
355 these are precisely the regions wherein we found non-conservative G interface substitutions
356 between fungal species that tolerate *CDC10* deletion and those that do not (Fig 4B). These
357 observations provide strong support for the idea that Gdm binding between the ScCdc3 α4 helix
358 and His262 mimics an ancestral evolutionary state and favors interaction with other similarly
359 disposed Cdc3 molecules.
360
361 **The GTPase properties of the Cdc3 subunit dictate septin subunit composition**
362 Our data support a model in which Gdm influences whether or not septin complexes incorporate a
363 central homodimer of mutant Cdc10 molecules by influencing whether the Cdc3 *trans* loop 1
364 contacts the Switch II loop of another Cdc3 molecule, or points toward the site where nucleotide is
365 normally bound by Cdc10. This model is reminiscent of the conclusions of a previous study, in which
366 we proposed that the conformation of the Switch II loop in Cdc12 biases choice of its G-dimer

367 partner (Cdc11 or Shs1)(58). In that study, we showed that a Switch II mutation in Cdc12 is sufficient
368 to bias partner choice. In an independent study (29), we found that a spontaneous mutation (D210G)
369 in the equivalent Switch II residue in Cdc3 restores the ability of Cdc3 to interact with a nucleotide-
370 free mutant Cdc10 at high temperatures. Like Gdm, the *cdc3(D210G)* mutation rescues the TS
371 phenotype of *cdc10(D182N)* cells, but unlike Gdm it does so by restoring, rather than bypassing,
372 incorporation of the mutant Cdc10 subunits; in other words, the Switch II mutation D210G biases
373 Cdc3 partner choice towards nucleotide-free Cdc10, whereas Gdm biases partner choice away from
374 it. Our model predicts that in *cdc3(D210G)* cells Gdm should be less able to exclude the mutant
375 Cdc10 than in cells expressing WT Cdc3, because the mutant Cdc3 Switch II will be unable to
376 accomplish the molecular contact(s) with the Cdc3 *trans* loop 1 that Gdm promotes. Indeed, Gdm
377 slightly reduced, but did not eliminate, Cdc10(D182N)-GFP localization to septin rings in
378 *cdc3(D210G)* cells (Fig 8A). These data are consistent with an important role for contacts between
379 the Switch II loop and the *trans* loop 1 during Cdc3 homodimerization promoted by Gdm.
380
381 Since Cdc12 is an active GTPase, and the Switch II changes conformation upon GTP hydrolysis,
382 we interpreted our previous results with Switch II-mutant Cdc12 as evidence that the Switch II
383 conformation normally "communicates" across the G interface the phosphorylation state of Cdc12's
384 bound nucleotide (58). We further bolstered this argument by mutating in Cdc12 a Thr residue in
385 the Switch I loop that is required for septin GTPase activity (39,58). Notably, Cdc3 lacks Thr in this
386 position. How could Gdm operate via Switch II conformation on Cdc3, a "dead" GTPase? We noticed
387 in our phylogenetic analysis of Cdc3 homologs in other fungal species that many possess the
388 "catalytic Thr" (S2 Fig). In fact, there was a perfect correlation between the presence of the catalytic
389 Thr (or Ser) and the α4 Arg whose Gdm group is presumably mimicked by Gdm in Cdc3 (S2 Fig).
390 Analogous to our model of Cdc12 G-partner choice via slow GTP hydrolysis (58), we reasoned that
391 in a species with an active "Cdc3" GTPase, a transient "Cdc3"•GTP molecule might prefer to

392 dimerize with “Cdc10” in that species, and “Cdc3”•GDP might prefer to form a homodimer,
393 bypassing “Cdc10” incorporation into septin complexes.
394
395 According to this model, because *Saccharomyces*, *Ashbya*, and *Kluyveromyces* species express
396 catalytically dead Cdc3 molecules, only Cdc3•GTP exists in these cells, and only Cdc10-containing
397 hetero-octamers are made. In *Aspergillus nidulans*, on the other hand, the Cdc3 homolog, AspB,
398 possesses the catalytic Thr (S2 Fig), and this species is known to produce a mix of octamers
399 containing AspD (the Cdc10 homolog) and AspD-less hexamers (59). We replaced the GTPase
400 domain of ScCdc3 (residues 95-341) with that of AspB (residues 6-234; S3 Fig) and assessed
401 Cdc10 incorporation into complexes by measuring the ratio of Cdc10-mCherry to Shs1-GFP in
402 septin rings of living cells. Consistent with our model, Cdc10-mCherry incorporation was markedly
403 reduced compared to cells with WT Cdc3 (Fig 8B), indicating that the GTPase properties of AspB
404 were sufficient to confer *Aspergillus*-like pathways of septin hetero-oligomer assembly, i.e., frequent
405 bypass of Cdc10 incorporation.
406
407 *S. cerevisiae* cells expressing the Cdc3-AspB chimera as the only source of Cdc3 were unable to
408 proliferate at 37ºC (Fig 8C). We hypothesized that this defect reflects misfolding at high temperature
409 of the Cdc3-AspB chimera to a conformation incapable of interacting with itself or with Cdc10, and
410 searched for spontaneous suppressors of the TS phenotype. We obtained a suppressor in which
411 proliferation at 37ºC was restored (Fig 8C). Sequencing the coding region of Cdc10 revealed a
412 single nucleotide change causing the amino acid substitution Q265H (Fig 8D); the Cdc3-AspB
413 chimera was unchanged. In most septin structures, His in this position makes a critical contact
414 across the G interface with a highly conserved Trp residue in the “Sep4” motif (3) (Fig 8E), the same
415 Trp we mutated in the *cdc3(W364A)* mutant (see Fig 2D). Since Gln replaces His here in ScCdc10
416 (and in the other fungal species with putatively GTPase-dead Cdc3 homologs; Table 2), the
417 Cdc3•GTP–Cdc10•GDP interface must involve a different kind of interaction. We interpret these

418 findings as evidence that stable association of Cdc10•GDP with GDP-bound Cdc3-AspB, rather
419 than the Cdc3•GTP with which Cdc10 co-evolved, requires His–Trp contacts between Sep4 motifs
420 of the sort found in other dimers between two GDP-bound septins. Indeed, incorporation of Cdc10-
421 mCherry into septin rings was partially restored in *cdc3-aspB cdc10(Q265H)* cells (Fig 8B). Finally,
422 Gdm was unable to fully rescue the TS phenotype of the *cdc3-aspB CDC10*$^{+}$ strain (Fig 8C), as
423 expected if the site of Gdm action is occluded by the α4 Arg present in the Cdc3-AspB chimera.
424 These data provide further support for the idea that during evolution ScCdc3 lost the ability to
425 hydrolyze GTP to GDP and, consequently, the option of assembling septin complexes without a
426 central Cdc10 homodimer.
427

Table 2. Co-variation among fungal species of the "catalytic Thr" in Cdc3 homologs and His in the Cdc10 *trans* loop 1.

Species	***Amino acid at position corresponding to ScCdc3 Lys181***	***Amino acid at position corresponding to ScCdc10 Lys155***	***Amino acid at position corresponding to ScCdc10 Gln265***
S. cerevisiae	Lys	Lys	Gln
A. gossypii	Lys	Lys	Gln
K. lactis	Lys	Lys	Gln
C. albicans	Ser	Gln	Gln
A. nidulans	Thr	His	His
C. cinerea	Thr	His	His
U. maydis	Thr	His	His
N. crassa	Thr	His	His
M. oryzae	Thr	His	His
F. graminearum	Thr	His	His
C. neoformans	Thr	His	His
S. pombe	Thr	His	His

428 The GTPase domains of Cdc3 and AspB are <50% identical, and differ at many more positions than
429 the five identified by our phylogenetic analysis as co-varying with the α4 Arg and the catalytic Thr
430 (S3 Fig). To ask if those five differences are sufficient to direct Cdc10 bypass during septin
431 assembly, we used CRISPR-Cas9 to cut the endogenous *CDC3* coding sequence and, via
432 homologous recombination, replace most of it with a "recoded" gene encoding the same polypeptide
433 sequence but using numerous synonymous codons, or with a similarly "recoded" gene additionally
434 encoding the five substitutions (P127E D128S K181T T302R Q306D). Recoding allowed us to

435 obtain transformants in which recombination occurred at the ends of our donor templates, rather
436 than in sequences immediately flanking the cut site, thus promoting incorporation of all five
437 substitutions. Nonetheless, we also obtained a transformant in which only two substitutions were
438 incorporated, T302R Q306D, and we included this strain in our subsequent analysis. The recoded
439 control strain and the *P127E D128S K181T T302R Q306D* and *T302R Q306D* mutant strains were
440 indistinguishable from the parental *CDC3*$^{+}$ strain in terms of growth at all tested temperatures, and
441 also with regard to the relative amounts of Cdc10-mCherry incorporated into septin rings (S4 Fig).
442 Thus, although we cannot rule out the possibility that recoding with synonymous codons alters Cdc3
443 co-translational folding in some way that masks effects of the amino acid changes we introduced, it
444 appears that additional sequence changes are needed to "reverse evolution" and restore the ability
445 of Cdc3 to homodimerize robustly *in vivo*.
446
447 DISCUSSION
448 **Septin G dimer partner selection by "tuning" the *trans* loop 1 His via α4 Arg or Gdm**
449 We propose that Gdm binding adjacent to ScCdc3 Thr302 provides molecular contacts that position
450 His262 to interact in *trans* with an Asp residue from a septin Switch II loop in a "GTP state", such
451 as that provided by another Cdc3•GTP. The spontaneous mutation we previously found to promote
452 Cdc3 homodimerization (23) alters a *trans* loop 1 residue immediately adjacent to Cdc3 His262,
453 Gly261. Val in this position probably also "tunes" the configuration of His262 to favor Cdc3
454 homodimerization via interaction with Cdc3 Asp201. Specific configurations of the Switch II loop
455 clearly dictate G dimer partner choice, as mutating the residue corresponding to Cdc3 Asp210
456 promotes both stable Cdc3 heterodimerization with nucleotide-free Cdc10 (29) and biased selection
457 of Shs1 by Cdc12 (58). Mutating a nearby Asp in the Switch II loop of human SEPT7 also allows
458 homodimerization when only a non-hydrolyzable GTP analog is available (60). "Tuning" by Gdm via
459 *cis* interactions presumably occurs prior to G dimerization, and is likely a transient event: once the
460 *trans* loop 1 His has engaged either the Switch II Asp or nucleotide (or nearby where nucleotide

461 normally binds, in the case of nucleotide-free mutant Cdc10), the Arg–His interaction probably need
462 not persist post-dimerization. It follows that Gdm may not remain bound to Cdc3 following G
463 dimerization, and thus falls under a broad definition of a “pharmacological” or “chemical” chaperone.
464
465 Since in otherwise WT cells Gdm promotes bypass of mutant Cdc10 molecules with substitutions
466 in various locations in the G interface and nucleotide-binding pocket (S1 Fig), but not WT Cdc10
467 (Fig 2), additional contacts between WT Cdc10•GDP and Cdc3•GTP likely favor Cdc3–Cdc10
468 heterodimerization over Cdc3 homodimerization despite the presence of Gdm. Poorer GdnHCl
469 rescue of *cdc10(G44D)* (P-loop mutant) relative to *cdc10(D182N)* (G4 mutant) and *cdc10(G100E)*
470 (Switch II mutant) (S1 Fig) may reflect a comparatively better ability of Cdc10(G44D) molecules to,
471 despite temperature-induced misfolding, occupy the Cdc3 G interface and resist exclusion, thereby
472 interfering with hexamer assembly. Bound nucleotide itself may provide the key contacts that
473 distinguish WT Cdc10 from the mutants, with Cdc10(G44D) subunits being more successful than
474 the other mutants at binding nucleotide. By contrast, swapping the GTPase domain of Cdc3 for that
475 of AspB was sufficient to promote bypass of WT Cdc10 (Fig 8B), consistent with the idea that
476 Cdc3•Gdm only partially mimics the ancestral homodimer configuration. Finally, introducing into
477 Cdc3 the five residues (including the catalytic Thr and α4 Arg) that are found in Cdc3 homologs in
478 species that tolerate loss of the Cdc10 homolog was unable to drive exclusion of Cdc10 from septin
479 complexes (S4 Fig). Similarly, Cdc12 natively possesses four of these five residues (S3 Fig), yet
480 forcing septin hexamer assembly via non-native Cdc12 homodimers (by deleting *SHS1* and *CDC11*)
481 results in *S. cerevisiae* cells that, like *cdc10*Δ, cannot proliferate at 37ºC (23). Clearly GTPase
482 activity and the presence of these residues is insufficient for robust septin homodimerization, and
483 additional changes are likely key.
484
485 **Insights into major events during septin evolution**

486 Although septins are absent from land plants, protein transport across the outer envelope
487 membrane of chloroplasts is mediated by TOC complexes containing a small GTPase subunit,
488 Toc34, that shares high structural homology to septins. Others have noted (56) that the septin *trans*
489 loop 1 is in a very similar position to a Toc34 interface loop that makes key contacts with nucleotide
490 bound by the partner protein across a homodimer interface (S5 Fig). In both pea (*Pisum sativum*)
491 and *Arabidopsis thaliana* an Arg residue in the Toc α4 helix projects towards the homodimer
492 interface, to within 5 Å of the *trans* loop 1 equivalent (S5 Fig). Arg in this position is conserved
493 among all Toc34 homologs (S4 Fig). We conclude that Arg-mediated α4 helix tuning of the *trans*
494 loop 1 for specific dimerization events across the nucleotide-binding-pocket-containing interface is
495 an evolutionarily ancient mechanism that predated the appearance of septins *per se*.
496
497 Following loss of the α4 Arg in the fungal lineage giving rise to *S. cerevisiae*, *A. gossypii*, and *K.*
498 *lactis*, the amino acid at the position equivalent to ScCdc3 Thr302 diverged rapidly. Ser or Ala
499 appear in its place in other species within the genus *Saccharomyces*, which share >86% sequence
500 identity with ScCdc3 (S6 Fig). By comparison, within the genus *Candida* Arg is invariant among 6
501 species sharing as little as 35% identity with *C. albicans* Cdc3 (S6 Fig). These observations are
502 consistent with the notion that Thr in this position does not make specific structural contributions to
503 septin assembly.
504
505 One clear prediction from this model is that in the two fungal lineages distinguished by the presence
506 or absence of the Cdc3 "catalytic" Thr, the Cdc10 subunit should have evolved differently, to
507 recognize in one case only Cdc3•GTP and, in the other, either Cdc3•GTP and Cdc3•GDP. Our
508 unbiased identification of the *cdc10(Q265H)* mutation in cells expressing the Cdc3-AspB chimera
509 provided one example of how Cdc10 adapted to interacting with a Cdc3 subunit "fixed" in the GTP-
510 bound state. Others previously noted (39) that ScCdc10 is unusual among septins in that it has Lys
511 rather than His in the *trans* loop 1. If the residue in this position acts to promote interaction with a G

512 dimer partner in a specific nucleotide state, this may explain why Lys in this position is shared by
513 AgCdc10 and KlCdc10, but not any of the Cdc10 homologs in the fungal species in which the Cdc3
514 homolog retains the "catalytic Thr" (Table 2). Co-variation of these residues likely reflects co-
515 evolution. S7A Fig illustrates a possible pathway of such changes during septin evolution.
516
517 Were Cdc10-less hexamers specifically selected against during evolution of a fungal lineage?
518 Compared to other closely-related fungi, *Ashbya*, *Kluyveromyces*, and *Saccharomyces* share little
519 in common with regard to the cellular functions in which septins are known to operate, such as
520 polarity, morphogenesis, cytokinesis, or sporulation. Hence it is hard to imagine how losing septin
521 hexamers could provide a specific selective advantage to a common ancestor, though this may
522 reflect our incomplete understanding of what septin hexamers do differently than septin octamers.
523
524 Many human cell types also natively produce both hexamers and octamers (61–65). Incorporation
525 of a subunit from the SEPT3 group (SEPT3, SEPT9, or SEPT12) appears to confer functions to
526 human hetero-octamers that hexamers lack, such as microtubule bundling (66), vesicle trafficking
527 in neurons (67), directing proper spermatogenesis (68), and membrane abscission at the end of
528 cytokinesis (69). Human and yeast septin octamers were thought to differ in where within the
529 complex the "extra" subunits incorporate, with SEPT3-group septins like SEPT9 occupying the
530 "terminal" positions at both octamer ends (65). However, two recent reports (70,71) suggest that in
531 fact SEPT3-group septins form a central homodimer flanked by SEPT7, with SEPT6 and SEPT2
532 occupying the penultimate and terminal positions, respectively. In this "revised" organization, the
533 GTPase-dead subunit position (the SEPT6 group) corresponds to that of Cdc12, and the Cdc3
534 position is occupied by SEPT7, an active GTPase (see S7B Fig). Notably, a mutation (S63N) that
535 doubles SEPT7 GTPase activity in vitro shifts assembly in vivo from primarily hetero-octamers to
536 smaller complexes (61), consistent with our model that septins in the GDP-bound state are prone
537 to homodimerization across the G interface and exclusion of intervening subunits.

538

539 Cdc10 and SEPT9 fall into one ancient evolutionary clade, whereas Cdc3, Cdc12, SEPT6 and
540 SEPT7 all appear to have distinct origins (4). Thus the loss of septin GTPase activity occurred
541 multiple times independently. By demonstrating that GTPase activity facilitates promiscuity during
542 dimerization, and thereby expands the repertoire of septin hetero-oligomers, our findings provide
543 the first molecular rationale for the evolution of GTPase-dead septins: to narrow the variety of
544 building blocks available for higher-order assemblies. A similar logic may explain the most famous
545 example of loss of GTPase activity of a cytoskeletal protein, that of the α subunit of the tubulin
546 heterodimer.

547

548 **Chemical rescue by guanidine hydrochloride *in vivo***

549 The ability of Gdm to occupy vacancies created by the mutation of Arg residues is well documented
550 *in vitro* for a wide variety of enzymes (40–42,55,72–77), but effects of GdnHCl on living cells were
551 limited to Gdm binding at sites in WT proteins or nucleic acids: in the ATP-binding pocket of Hsp104
552 and its relatives (78), in the intracellular pore of voltage-gated potassium channels (79), in the
553 enteroviral 2C protein (80), and, most recently, in bacterial riboswitches that sense intracellular Gdm
554 and induce a cellular response to detoxify it (81). The function of a rationally-designed Arg-mutant
555 kinase can be rescued *in vitro* by GdnHCl (82), and the same mutant is rescued by imidazole *in vivo*
556 (83), but our findings that GdnHCl can functionally replace an Arg in Cdc3 represent the first
557 documented case of "chemical rescue" by GdnHCl *in vivo*. In yeast cells cultured in 1 mM GdnHCl
558 the intracellular concentration is ~20 mM (84); under such conditions Gdm likely binds to hundreds
559 or thousands of proteins, with few adverse effects. Indeed, GdnHCl is approved by the Food and
560 Drug Administration of the USA for use in humans, and at low doses has few serious side effects
561 (85). Exploiting the ability of Gdm to replace Arg in living cells represents a compelling area for
562 future research, particularly as a possible therapeutic "pharmacoperone" (86). Finally, given the
563 evidence that bacteria evolved ways to manage intracellular Gdm (including actively exporting it

564 (87)), Gdm could, like the naturally occurring osmolyte trimethylamine N-oxide (88) and the protein
565 chaperone Hsp90 (89), influence evolution by buffering against the phenotypic consequences of
566 mutations.
567

568 MATERIALS AND METHODS

569 **Fungal strains and plasmids**

570 The sources and genotypes for all fungal strains and plasmids are listed in the Supporting
571 Information (S1 Table). Primer and synthetic gene sequences are listed in S2 Table. Yeast were
572 transformed using the Frozen-EZ Yeast Transformation II Kit (Zymo Research). Genetic
573 manipulations were otherwise performed according to standard methods (90), except for the
574 creation of the *cdc3-aspB* chimera and the *CDC3(P127E D128S K181T T302R Q306D)* and
575 *CDC3(T302R Q306D)* strains and associated "recoded" control strain, which were made in yeast
576 strain JTY5397 using CRISPR-Cas9 cleavage of the *CDC3* locus and repair with PCR products as
577 donor templates, following an established protocol (91) and using plasmid pEM-CDC3-CRISPR1, a
578 gift of Ed Marcotte, which encodes Cas9 and a guide RNA targeting nucleotides 1039-1069 of the
579 *CDC3* ORF (5' GATATTGTAGAGAACTACAG 3'). To create the donor template for the *cdc3-aspB*
580 chimera, a portion of the *aspB* coding sequence, the *aspB* plasmid pRL10, which was a gift of
581 Michelle Momany and is based on the yeast two-hybrid vector pGBKT7 (Takara Bio/Clontech), was
582 used as template for a PCR reaction with Q5 polymerase (New England Biolabs) and primers
583 Cdc3AspBfw and Cdc3AspBextend1 according to the polymerase manufacturer's instructions. The
584 resulting product, which included the sequence encoding part of AspB flanked by *CDC3* sequences,
585 was used as template for a second Q5 reaction with primers Cdc3AspBfw and
586 Cdc3GTPase_extend2, in order to extend the *CDC3* homology to span the site of the Cas9 cut. To
587 create the donor template for the *CDC3(P127E D128S K181T T302R Q306D)* strain and its
588 "recoded" control, an 870-nucleotide segment of the Cdc3 ORF corresponding to the GTPase
589 domain was synthesized (Integrated DNA Technologies) with multiple synonymous codons
590 replacing the native sequence (S2 Table), representing 67 nucleotide changes but no amino acid
591 substitutions. An otherwise identical sequence also including the *P127E D128S K181T T302R*
592 *Q306D* mutations was also synthesized (S2 Table). Donor template PCRs were done with Q5 and

593 primers G1KTTRQDfw and Cdc3recodere (S2 Table). Transformants were screened by PCR of the
594 *CDC3* locus and subsequent sequencing. Low-copy, *LEU2*-marked *CDC3* or *CDC3-GFP* plasmids
595 were pFM831 (39) or pML109 (26). Plasmids YCpHLcdc3(T302R)-GFP and YCpHLcdc3(T302V)-
596 GFP were made via site-directed mutagenesis using template plasmid pML109 by Keyclone
597 Technologies (San Marcos, CA). Low-copy, *kanMX*-marked plasmid YCpK-Cdc10-1-GFP, encoding
598 *cdc10(D182N)-GFP*, was described previously (30).
599
600 **Media and additives**
601 *S. cerevisiae* media: Rich growth medium was YPD (1% yeast extract (#Y20020, Research
602 Products International Corp., Mount Prospect, IL), 2% peptone (#P20241, RPI Corp.), 2% dextrose
603 (#G32045, RPI Corp.)). Synthetic growth medium was based on YC (0.1 g/L Arg, Leu, Lys, Thr, Trp
604 and uracil; 0.05 g/L Asp, His, Ile, Met, Phe, Pro, Ser, Tyr and Val; 0.01 g/L adenine; 1.7 g/L Yeast
605 Nitrogen Base (YNB) without amino acids or ammonium sulfate; 5 g/L ammonium sulfate; 2%
606 dextrose) with individual components (from Sigma Aldrich, St. Louis, MO, or RPI Corp.) eliminated
607 as appropriate for plasmid selection. For solid media, agar (#A20030, RPI Corp.) was added to 2%.
608 For counterselection against *URA3*, 5-fluoro-orotic acid monohydrate (#F5050, United States
609 Biological, Salem, MA) was added to modified YC medium (1 g/L Pro in place of ammonium sulfate,
610 0.02 g/L uracil) to final 0.6 g/L. For counterselection against *LYS2*, α-aminoadipate (#A1374-09, US
611 Biological) at 2 g/L replaced ammonium sulfate in YC medium containing only YNB, uracil, His, Leu,
612 Lys, Met, Trp, and dextrose. G418 sulfate (Geneticin®, #G1000, US Biological) was added to YPD
613 at 200 μg/mL for selection of *kanMX*.
614
615 *A. gossypii* media: Ashbya strains were grown in 10 mL Ashbya Full Medium (AFM, 1% casein
616 peptone, 1% yeast casein extract, 2% dextrose and 0.1% myo-inositol) containing ampicillin (100
617 μg/mL), CloNAT (50 μg/mL) and G-418 (200 μg/mL). For imaging, cells were washed into 2X low-

618 fluorescence minimal medium (per liter: 3.4 g YNB without amino acids or ammonium sulfate, 2 g
619 Asp, 2 g myo-inositol, 40 g dextrose, 20 mg adenine, 21 g 3-(N-morpholino)propanesulfonic acid
620 (MOPS), pH adjusted to 7.0 with sodium hydroxide).
621
622 GdnHCl (#G4505, Sigma Aldrich, St. Louis, MO), ArgHCl (#A5131, Sigma Aldrich), aminoguanidine
623 HCl (#sc-202931, Santa Cruz Biotechnology, Santa Cruz, CA) and N-ethylguanidine HCl (#sc-
624 269833, Santa Cruz Biotechnology) were dissolved in water.
625
626 **Growth curves**
627 Growth curves were generated using a Cytation 3 plate reader (BioTek, Winooski, Vermont) as
628 described previously (92) using a starting overnight culture of the *cdc10(D182N)* strain CBY06417
629 grown at 22ºC prior to dilution into 200 µl YPD medium in each well.
630
631 **Immunofluorescence**
632 Immunofluoresence was performed as described previously (93) using an anti-Cdc11 primary
633 antibody (#sc7170, Santa Cruz Biotechnology, Santa Cruz, CA) and Alexa-Fluor 488-labeled anti-
634 rabbit secondary antibody (#20012, Biotium, Inc., Fremont, CA) at a 1:5000 and 1:1000 dilution,
635 respectively.
636
637 **Electron microscopy**
638 Cells cultured at 37°C in YPD medium with 3 mM GdnHCl were collected by vacuum filtration and
639 vitrified by high pressure freezing using a HPM100 (Leica Microsystems, Wetzlar, Germany)
640 apparatus. The frozen cells were cryo-substituted using a Leica ASF2 device in a medium
641 containing osmium tetroxide (1%), water (5%) and uranyl acetate (0.1%) in acetone using a protocol
642 described elsewhere (94). The cells were embedded into Epon before being sectioned into 50 nm

643 sections using an ultramicrotome UC6 (Leica) equipped with a 4.5 mm diamond knife (Diatome,
644 Hatfield, PA). The resulting sections were deposited onto copper electron microscopy grids (mesh
645 size of 100). The images were collected with a 120 kV Lab6 microscope (Technai Spirit, FEI,
646 Eindhoven, Netherlands) equipped with a CCD Quemesa camera (Olympus, Tokyo, Japan).
647

648 **Fluorescence microscopy**

649 All images of *S. cerevisiae* were captured using an EVOSfl all-in-one microscope (Advanced
650 Microscopy Group, Mill Creek, Washington) using a 60X objective and Texas Red, RFP, or GFP
651 LED/filter cubes, as described previously (30). Bud neck fluorescence was quantified using line
652 scans as described previously (30,58). Intensity values or ratios thereof were plotted using
653 GraphPad Prism 8.0, using the medium smoothing (kernel density) setting for violin plots. When
654 necessary for presentation, images were inverted and brightness- and contrast-adjusted using
655 Adobe Photoshop (Adobe Systems Incorporated, San Jose, California), always the same way for
656 every image of the same type.
657

658 *Ashbya* cells in minimal low-fluorescence medium were mounted onto 2% agarose gel pads and
659 the edges were sealed with Valap (a 1:1:1 mixture of vaseline, lanolin, and paraffin). Images were
660 acquired using a Zeiss Axioimager-M1 upright light microscope (Carl Zeiss, Jenna, Germany)
661 equipped with a Plan-Apochromat 63X/1.4 numerical aperture oil objective and an Exfo X-Cite 120
662 lamp. Fluorescence imaging was performed using Zeiss 38HE filter cubes (GFP). Images were
663 acquired using an Orca-AG charge-coupled device (CCD) camera driven by μManager.
664

665 **Expression, purification and analysis of recombinant septins**

666 BL21 Star™(DE3) *E. coli* cells (ThermoFisher Scientific # C601003) were transformed with plasmids
667 pMVB121 (encoding 6xHis-Cdc12) and pMVB133 (encoding untagged Cdc3 and Cdc11) and grown

668 overnight in 3 mL LB medium (per L: 10 g tryptone, 5 g yeast extract, 10 g NaCl) with ampicillin (50
669 μg/mL), chloramphenicol (34 μg/mL), and varying amounts of GdnHCl (from 0 mM to 96 mM) at
670 37ºC in glass culture tubes with agitation. Growth was assessed qualitatively and was equivalent
671 for all cultures, so 100 mM was chosen as the concentration for subsequent experiments. 1-L LB
672 cultures with ampicillin, chloramphenicol and with or without 100 mM GdnHCl were grown at 37ºC
673 with shaking to OD_{600} between 0.6 and 1.0, at which point IPTG was added to 0.1 mM and the
674 culture was incubated overnight. Cells were collected by centrifugation, resuspended in a minimal
675 volume of lysis buffer (300 mM NaCl, 2 mM $MgCl_2$, 40 μM GTP, 1 mM EDTA, 5 mM β-
676 mercaptoethanol, 0.5% Tween-20, 12% glycerol, 50 mM Tris-HCl, pH 8.0) and frozen by dripping
677 into liquid nitrogen. Cells were thawed in 30 mL lysis buffer containing protease inhibitors (Complete
678 EDTA-free, Roche #11836170001) and lysed with a French press. Lysates were clarified by
679 centrifugation at 12,000xg at 4ºC and mixed with 200 μL of a slurry of Ni^{2+}-NTA agarose (Qiagen
680 #30210) that had been equilibrated in lysis buffer. After rotating for 1 hour at 4ºC, beads were
681 collected by centrifugation, washed two times with 5 mL of 300 mM NaCl, 20 mM imidazole, 0.1%
682 Tween-20, and 50 mM Tris-HCl, pH 8.0. The beads were poured into a column and the septin
683 complex was eluted in fractions from the beads with 500 mM NaCl, 40 μM GTP, 500 mM imidazole,
684 50 mM Tris-HCl, pH 8.0. Aliquots of fractions were analyzed by SDS-PAGE and Coomassie
685 staining, and imidazole was removed from the fraction containing the peak of septin complex via
686 buffer exchange into 500 mM NaCl, 40 μM GTP, 50 mM Tris-HCl, pH 8.0 using a PD-10 column
687 (GE Healthcare LifeSciences # 17085101). For the complex produced in the presence of GdnHCl,
688 100 mM GdnHCl was included in all buffers. The purified complex in high salt was pre-cleared by
689 centrifugation at 100,000xg for 1 hour at 4ºC. To initiate filament polymerization, 200 μL was diluted
690 5-fold with a low-salt buffer (40 μM GTP, 40 μM $MgCl_2$, 50 mM Tris-HCl pH 8.0 with or without 100
691 mM GdnHCl) and incubated at 4ºC overnight before centrifugation at 100,000xg for 1 hour at 4ºC.
692 The supernatant was carefully removed and the pelleted material was resuspended in SDS-PAGE

693 loading buffer. Molecular weight marker was Chameleon Duo Pre-stained Protein Ladder, LiCor
694 #928-60000.
695
696 **Immunoblotting**
697 SDS-PAGE gels were transferred to low-fluorescence polyvinylidene difluoride membrane (Bio-Rad
698 #162-0264) with a semi-dry transfer device (Bio-Rad # 1703940) according to the manufacturer's
699 instructions. The membrane was blocked with Odyssey Blocking Buffer (LiCor # 927-50000) and
700 incubated with anti-Cdc11 primary antibody (#sc7170, Santa Cruz Biotechnology, Santa Cruz, CA)
701 and Alexa-Fluor 488-labeled anti-rabbit secondary antibody (Anti Rabbit IgG DyLight 800, Cell
702 Signaling Technology #5257) at a 1:1,000 and 1:10,000 dilution, respectively. After washing, the
703 membrane was scanned with an infrared scanner (LiCor Odyssey).
704
705 ***In silico* docking, structure prediction, and analysis**
706 Visualization and rendering of structures in PDB format was performed using MacPyMol
707 (Schrödinger, New York, NY). Residues within 5 Å of other residues were identified using the
708 "around" command. Structure prediction for ScCdc3 was performed using the I-TASSER server
709 (http://zhanglab.ccmb.med.umich.edu/I-TASSER/) (95) and ScCdc3 sequence truncated to amino
710 acids 116-411 to match the template model, SEPT2•GppNHp (PDB 3FTQ). Molecular docking was
711 performed using a local installation of AutoDock Vina (96) via Chimera 1.11
712 (http://www.rbvi.ucsf.edu/chimera) (97), using a search volume containing the entire "receptor"
713 model.
714
715 **Sequence alignments**
716 Multiple alignments were performed using the COBALT tool at the NCBI server
717 (https://www.ncbi.nlm.nih.gov/tools/cobalt/) or, for sequences of yeast species not available via

718 NCBI, using the "Fungal Alignment" function at the Yeast Genome Database (98). In some cases,
719 sequences obtained via the Yeast Genome Database were aligned with other sequences via
720 COBALT.
721
722 **DNA sequencing**
723 Genomic DNA from the *cdc3-AspB* suppressor strain was isolated as described previously and used
724 as template in Q5 PCR reactions with primers 5'cdc3fw and 3'cdc3re, or 5'cdc10fw and 3'cdc10re
725 performed according to the polymerase manufacturer's instructions. Following treatment with
726 alkaline phosphatase and Exonuclease I (Thermo Scientific Fermentas), the purified PCR product
727 was directly sequenced at the sequencing facility of the Barbara Davis Center for Childhood Obesity,
728 with the same primers used for amplification and, for *CDC10*, with primer cdc10midfw. To confirm
729 correct strain construction sequences of other loci were performed in an equivalent manner with
730 appropriate primers (S2 Table).
731
732 **Choice of sample sizes and statistical analysis**
733 Sample sizes (*n*, number of cells) for fluorescence microscopy were chosen based on our ability to
734 detect decreases in bud neck localization in our previous studies (30,58). Analysis of effect sizes
735 and generation of effect size plots were performed using DABEST (data analysis with bootstrap-
736 coupled estimation) (99) via the online server at http://www.estimationstats.com. Other violin plots
737 were generated with Prism 8.0 (Graphpad) using the "medium" smoothing/kernel density setting.
738
739 ACKNOWLEDGEMENTS
740 We thank Michelle Momany (University of Georgia, USA) for fruitful discussions about septin
741 evolution and sharing unpublished reagents. The UCSF Chimera software package is developed
742 by the Resource for Biocomputing, Visualization, and Informatics at the University of California, San

744 Francisco (supported by NIGMS P41-GM103311). We also acknowledge the PICT-IBiSA (Institut
745 Curie, Paris).
746

747 REFERENCES

748 1. Onishi M, Pringle JR. The nonopisthokont septins: How many there are, how little we know about
749 them, and how we might learn more. Methods Cell Biol. 2016;136:1–19.

750 2. Nishihama R, Onishi M, Pringle JR. New insights into the phylogenetic distribution and
751 evolutionary origins of the septins. Biol Chem. 2011 Aug;392(8–9):681–7.

752 3. Pan F, Malmberg RL, Momany M. Analysis of septins across kingdoms reveals orthology and new
753 motifs. BMC Evol Biol. 2007;7:103.

754 4. Auxier B, Dee J, Berbee ML, Momany M. Diversity of opisthokont septin proteins reveals
755 structural constraints and conserved motifs. BMC Evol Biol. 2019 07;19(1):4.

756 5. Mostowy S, Cossart P. Septins: the fourth component of the cytoskeleton. Nat Rev Mol Cell Biol.
757 2012 Mar;13(3):183–94.

758 6. Oh Y, Bi E. Septin structure and function in yeast and beyond. Trends Cell Biol. 2011
759 Mar;21(3):141–8.

760 7. Fung KYY, Dai L, Trimble WS. Cell and molecular biology of septins. Int Rev Cell Mol Biol.
761 2014;310:289–339.

762 8. Dolat L, Hu Q, Spiliotis ET. Septin functions in organ system physiology and pathology. Biol Chem.
763 2014 Feb;395(2):123–41.

764 9. Saarikangas J, Barral Y. The emerging functions of septins in metazoans. EMBO Rep. 2011
765 Nov;12(11):1118–26.

766 10. Nakahira M, Macedo JNA, Seraphim TV, Cavalcante N, Souza TACB, Damalio JCP, et al. A draft of
767 the human septin interactome. PloS One. 2010;5(11):e13799.

768 11. Versele M, Gullbrand B, Shulewitz MJ, Cid VJ, Bahmanyar S, Chen RE, et al. Protein-protein
769 interactions governing septin heteropentamer assembly and septin filament organization in
770 Saccharomyces cerevisiae. Mol Biol Cell. 2004 Oct;15(10):4568–83.

771 12. Farkasovsky M, Herter P, Voss B, Wittinghofer A. Nucleotide binding and filament assembly of
772 recombinant yeast septin complexes. Biol Chem. 2005 Jul;386(7):643–56.

773 13. Leipe DD, Wolf YI, Koonin EV, Aravind L. Classification and evolution of P-loop GTPases and
774 related ATPases. J Mol Biol. 2002 Mar 15;317(1):41–72.

775 14. Sirajuddin M, Farkasovsky M, Hauer F, Kühlmann D, Macara IG, Weyand M, et al. Structural
776 insight into filament formation by mammalian septins. Nature. 2007 Sep 20;449(7160):311–5.

777 15. Bertin A, McMurray MA, Grob P, Park S-S, Garcia G, Patanwala I, et al. Saccharomyces cerevisiae
778 septins: supramolecular organization of heterooligomers and the mechanism of filament
779 assembly. Proc Natl Acad Sci U S A. 2008 Jun 17;105(24):8274–9.

780 16. Mitchison TJ, Field CM. Cytoskeleton: what does GTP do for septins? Curr Biol CB. 2002 Nov
781 19;12(22):R788-790.

782 17. Pablo-Hernando ME, Arnaiz-Pita Y, Tachikawa H, del Rey F, Neiman AM, Vázquez de Aldana CR.
783 Septins localize to microtubules during nutritional limitation in Saccharomyces cerevisiae. BMC
784 Cell Biol. 2008;9:55.

785 18. De Virgilio C, DeMarini DJ, Pringle JR. SPR28, a sixth member of the septin gene family in
786 Saccharomyces cerevisiae that is expressed specifically in sporulating cells. Microbiol Read Engl.
787 1996 Oct;142 (Pt 10):2897–905.

788 19. Fares H, Goetsch L, Pringle JR. Identification of a developmentally regulated septin and
789 involvement of the septins in spore formation in Saccharomyces cerevisiae. J Cell Biol. 1996
790 Feb;132(3):399–411.

791 20. Heasley LR, McMurray MA. Roles of septins in prospore membrane morphogenesis and spore
792 wall assembly in Saccharomyces cerevisiae. Mol Biol Cell. 2016 Feb 1;27(3):442–50.

793 21. Garcia G, Finnigan GC, Heasley LR, Sterling SM, Aggarwal A, Pearson CG, et al. Assembly,
794 molecular organization, and membrane-binding properties of development-specific septins. J Cell
795 Biol. 2016 Feb 29;212(5):515–29.

796 22. Kulak NA, Pichler G, Paron I, Nagaraj N, Mann M. Minimal, encapsulated proteomic-sample
797 processing applied to copy-number estimation in eukaryotic cells. Nat Methods. 2014
798 Mar;11(3):319–24.

799 23. McMurray MA, Bertin A, Garcia G 3rd, Lam L, Nogales E, Thorner J. Septin filament formation is
800 essential in budding yeast. Dev Cell. 2011 Apr 19;20(4):540–9.

801 24. Hartwell LH. Genetic control of the cell division cycle in yeast. IV. Genes controlling bud
802 emergence and cytokinesis. Exp Cell Res. 1971 Dec;69(2):265–76.

803 25. McMurray MA. Assays for genetic dissection of septin filament assembly in yeast, from de novo
804 folding through polymerization. Methods Cell Biol. 2016;136:99–116.

805 26. Nagaraj S, Rajendran A, Jackson CE, Longtine MS. Role of nucleotide binding in septin-septin
806 interactions and septin localization in Saccharomyces cerevisiae. Mol Cell Biol. 2008
807 Aug;28(16):5120–37.

808 27. Iwase M, Luo J, Bi E, Toh-e A. Shs1 plays separable roles in septin organization and cytokinesis in
809 Saccharomyces cerevisiae. Genetics. 2007 Sep;177(1):215–29.

810 28. Garcia G 3rd, Bertin A, Li Z, Song Y, McMurray MA, Thorner J, et al. Subunit-dependent
811 modulation of septin assembly: budding yeast septin Shs1 promotes ring and gauze formation. J
812 Cell Biol. 2011 Dec 12;195(6):993–1004.

813 29. Weems AD, Johnson CR, Argueso JL, McMurray MA. Higher-Order Septin Assembly Is Driven by
814 GTP-Promoted Conformational Changes: Evidence From Unbiased Mutational Analysis in
815 Saccharomyces cerevisiae. Genetics. 2014 Mar;196(3):711–27.

816 30. Johnson CR, Weems AD, Brewer JM, Thorner J, McMurray MA. Cytosolic chaperones mediate
817 quality control of higher-order septin assembly in budding yeast. Mol Biol Cell. 2015 Feb 11;

818 31. Sweeny EA, Shorter J. Mechanistic and Structural Insights into the Prion-Disaggregase Activity of
819 Hsp104. J Mol Biol. 2016 May 8;428(9 Pt B):1870–85.

820 32. Derkatch IL, Bradley ME, Zhou P, Chernoff YO, Liebman SW. Genetic and environmental factors
821 affecting the de novo appearance of the [PSI+] prion in Saccharomyces cerevisiae. Genetics. 1997
822 Oct;147(2):507–19.

823 33. Jung G, Masison DC. Guanidine hydrochloride inhibits Hsp104 activity in vivo: a possible
824 explanation for its effect in curing yeast prions. Curr Microbiol. 2001 Jul;43(1):7–10.

825 34. Erives AJ, Fassler JS. Metabolic and chaperone gene loss marks the origin of animals: evidence for
826 Hsp104 and Hsp78 chaperones sharing mitochondrial enzymes as clients. PloS One.
827 2015;10(2):e0117192.

828 35. Tuite MF, Mundy CR, Cox BS. Agents that cause a high frequency of genetic change from [psi+] to
829 [psi-] in Saccharomyces cerevisiae. Genetics. 1981 Aug;98(4):691–711.

830 36. Longtine MS, Bi E. Regulation of septin organization and function in yeast. Trends Cell Biol. 2003
831 Aug;13(8):403–9.

832 37. Bolanos-Garcia VM, Davies OR. Structural analysis and classification of native proteins from E.
833 coli commonly co-purified by immobilised metal affinity chromatography. Biochim Biophys Acta
834 BBA - Gen Subj. 2006 Sep 1;1760(9):1304–13.

835 38. Saito Y, Wada A. Comparative study of GuHCl denaturation of globular proteins. II. A
836 phenomenological classification of denaturation profiles of 17 proteins. Biopolymers. 1983
837 Sep;22(9):2123–32.

838 39. Sirajuddin M, Farkasovsky M, Zent E, Wittinghofer A. GTP-induced conformational changes in
839 septins and implications for function. Proc Natl Acad Sci U S A. 2009 Sep 29;106(39):16592–7.

840 40. Baldwin E, Baase WA, Zhang X j, Feher V, Matthews BW. Generation of ligand binding sites in T4
841 lysozyme by deficiency-creating substitutions. J Mol Biol. 1998 Mar 27;277(2):467–85.

842 41. Dugdale ML, Vance ML, Wheatley RW, Driedger MR, Nibber A, Tran A, et al. Importance of Arg-
843 599 of β-galactosidase (Escherichia coli) as an anchor for the open conformations of Phe-601 and
844 the active-site loop. Biochem Cell Biol Biochim Biol Cell. 2010 Dec;88(6):969–79.

845 42. Phillips MA, Hedstrom L, Rutter WJ. Guanidine derivatives restore activity to carboxypeptidase
846 lacking arginine-127. Protein Sci Publ Protein Soc. 1992 Apr;1(4):517–21.

847 43. Vargas-Muñiz JM, Renshaw H, Richards AD, Lamoth F, Soderblom EJ, Moseley MA, et al. The
848 Aspergillus fumigatus septins play pleiotropic roles in septation, conidiation, and cell wall stress,
849 but are dispensable for virulence. Fungal Genet Biol FG B. 2015 Aug;81:41–51.

850 44. Hernández-Rodríguez Y, Hastings S, Momany M. The septin AspB in Aspergillus nidulans forms
851 bars and filaments and plays roles in growth emergence and conidiation. Eukaryot Cell. 2012
852 Mar;11(3):311–23.

853 45. Warenda AJ, Konopka JB. Septin function in Candida albicans morphogenesis. Mol Biol Cell. 2002
854 Aug;13(8):2732–46.

855 46. Kozubowski L, Heitman J. Septins enforce morphogenetic events during sexual reproduction and
856 contribute to virulence of Cryptococcus neoformans. Mol Microbiol. 2010 Feb;75(3):658–75.

857 47. Chen A, Xie Q, Lin Y, Xu H, Shang W, Zhang J, et al. Septins are involved in nuclear division,
858 morphogenesis and pathogenicity in Fusarium graminearum. Fungal Genet Biol FG B. 2016
859 Sep;94:79–87.

860 48. Berepiki A, Read ND. Septins are important for cell polarity, septation and asexual spore
861 formation in Neurospora crassa and show different patterns of localisation at germ tube tips.
862 PloS One. 2013;8(5):e63843.

863 49. An H, Morrell JL, Jennings JL, Link AJ, Gould KL. Requirements of fission yeast septins for complex
864 formation, localization, and function. Mol Biol Cell. 2004 Dec;15(12):5551–64.

865 50. Alvarez-Tabarés I, Pérez-Martín J. Septins from the phytopathogenic fungus Ustilago maydis are
866 required for proper morphogenesis but dispensable for virulence. PloS One. 2010;5(9):e12933.

867 51. Dagdas YF, Yoshino K, Dagdas G, Ryder LS, Bielska E, Steinberg G, et al. Septin-mediated plant cell
868 invasion by the rice blast fungus, Magnaporthe oryzae. Science. 2012 Jun 22;336(6088):1590–5.

869 52. Shioya T, Nakamura H, Ishii N, Takahashi N, Sakamoto Y, Ozaki N, et al. The Coprinopsis cinerea
870 septin Cc.Cdc3 is involved in stipe cell elongation. Fungal Genet Biol FG B. 2013 Oct;58–59:80–
871 90.

872 53. Rippert D, Heinisch JJ. Investigation of the role of four mitotic septins and chitin synthase 2 for
873 cytokinesis in Kluyveromyces lactis. Fungal Genet Biol FG B. 2016 Sep;94:69–78.

874 54. Helfer H, Gladfelter AS. AgSwe1p Regulates Mitosis in Response to Morphogenesis and Nutrients
875 in Multinucleated Ashbya gossypii Cells. Mol Biol Cell. 2006 Oct 1;17(10):4494–512.

876 55. Rynkiewicz MJ, Seaton BA. Chemical rescue by guanidine derivatives of an arginine-substituted
877 site-directed mutant of Escherichia coli ornithine transcarbamylase. Biochemistry. 1996 Dec
878 17;35(50):16174–9.

879 56. Weirich CS, Erzberger JP, Barral Y. The septin family of GTPases: architecture and dynamics. Nat
880 Rev Mol Cell Biol. 2008 Jun;9(6):478–89.

881 57. Pinto APA, Pereira HM, Zeraik AE, Ciol H, Ferreira FM, Brandão-Neto J, et al. Filaments and
882 fingers: Novel structural aspects of the single septin from Chlamydomonas reinhardtii. J Biol
883 Chem. 2017 Jun 30;292(26):10899–911.

884 58. Weems A, McMurray M. The step-wise pathway of septin hetero-octamer assembly in budding
885 yeast. eLife. 2017 25;6.

886 59. Hernández-Rodríguez Y, Masuo S, Johnson D, Orlando R, Smith A, Couto-Rodriguez M, et al.
887 Distinct Septin Heteropolymers Co-Exist during Multicellular Development in the Filamentous
888 Fungus Aspergillus nidulans. PloS One. 2014;9(3):e92819.

889 60. Zent E, Wittinghofer A. Human septin isoforms and the GDP-GTP cycle. Biol Chem. 2014
890 Feb;395(2):169–80.

891 61. Abbey M, Hakim C, Anand R, Lafera J, Schambach A, Kispert A, et al. GTPase domain driven
892 dimerization of SEPT7 is dispensable for the critical role of septins in fibroblast cytokinesis. Sci
893 Rep. 2016 Jan 28;6:20007.

894 62. Sellin ME, Holmfeldt P, Stenmark S, Gullberg M. Microtubules support a disk-like septin
895 arrangement at the plasma membrane of mammalian cells. Mol Biol Cell. 2011 Dec;22(23):4588–
896 601.

897 63. Sellin ME, Sandblad L, Stenmark S, Gullberg M. Deciphering the rules governing assembly order
898 of mammalian septin complexes. Mol Biol Cell. 2011 Sep;22(17):3152–64.

899 64. Sellin ME, Stenmark S, Gullberg M. Cell type-specific expression of SEPT3-homology subgroup
900 members controls the subunit number of heteromeric septin complexes. Mol Biol Cell. 2014
901 May;25(10):1594–607.

902 65. Kim MS, Froese CD, Estey MP, Trimble WS. SEPT9 occupies the terminal positions in septin
903 octamers and mediates polymerization-dependent functions in abscission. J Cell Biol. 2011 Nov
904 28;195(5):815–26.

905 66. Bai X, Bowen JR, Knox TK, Zhou K, Pendziwiat M, Kuhlenbäumer G, et al. Novel septin 9 repeat
906 motifs altered in neuralgic amyotrophy bind and bundle microtubules. J Cell Biol. 2013 Dec
907 23;203(6):895–905.

908 67. Karasmanis EP, Phan C-T, Angelis D, Kesisova IA, Hoogenraad CC, McKenney RJ, et al. Polarity of
909 Neuronal Membrane Traffic Requires Sorting of Kinesin Motor Cargo during Entry into Dendrites
910 by a Microtubule-Associated Septin. Dev Cell. 2018 Jul 16;46(2):204-218.e7.

911 68. Kuo Y-C, Shen Y-R, Chen H-I, Lin Y-H, Wang Y-Y, Chen Y-R, et al. SEPT12 orchestrates the
912 formation of mammalian sperm annulus by organizing core octameric complexes with other
913 SEPT proteins. J Cell Sci. 2015 Mar 1;128(5):923–34.

914 69. Estey MP, Ciano-Oliveira CD, Froese CD, Bejide MT, Trimble WS. Distinct roles of septins in
915 cytokinesis: SEPT9 mediates midbody abscission. J Cell Biol. 2010 Nov 15;191(4):741–9.

916 70. Soroor F, Kim MS, Palander O, Balachandran Y, Collins R, Benlekbir S, et al. Revised subunit order
917 of mammalian septin complexes explains their in vitro polymerization properties. bioRxiv. 2019
918 Mar 7;569871.

919 71. Mendonça DC, Macedo JN, Itri R, Guimaraes SL, Silva FLB da, Cassago A, et al. Repositioning
920 septins within the core particle. bioRxiv. 2019 Mar 8;569251.

921 72. Boehlein SK, Walworth ES, Richards NG, Schuster SM. Mutagenesis and chemical rescue indicate
922 residues involved in beta-aspartyl-AMP formation by Escherichia coli asparagine synthetase B. J
923 Biol Chem. 1997 May 9;272(19):12384–92.

924 73. Lehoux IE, Mitra B. Role of arginine 277 in (S)-mandelate dehydrogenase from Pseudomonas
925 putida in substrate binding and transition state stabilization. Biochemistry. 2000 Aug
926 22;39(33):10055–65.

927 74. Hung JE, Fogle EJ, Garg N, Chekan JR, Nair SK, van der Donk WA. Chemical rescue and inhibition
928 studies to determine the role of Arg301 in phosphite dehydrogenase. PloS One.
929 2014;9(1):e87134.

930 75. Goedl C, Nidetzky B. The phosphate site of trehalose phosphorylase from Schizophyllum
931 commune probed by site-directed mutagenesis and chemical rescue studies. FEBS J. 2008
932 Mar;275(5):903–13.

933 76. Barnett SA, Amyes TL, Wood BM, Gerlt JA, Richard JP. Activation of R235A mutant orotidine 5'-
934 monophosphate decarboxylase by the guanidinium cation: effective molarity of the cationic side
935 chain of Arg-235. Biochemistry. 2010 Feb 9;49(5):824–6.

936 77. Guillén Schlippe YV, Hedstrom L. Guanidine derivatives rescue the Arg418Ala mutation of
937 Tritrichomonas foetus IMP dehydrogenase. Biochemistry. 2005 Dec 20;44(50):16695–700.

938 78. Zeymer C, Werbeck ND, Schlichting I, Reinstein J. The molecular mechanism of Hsp100
939 chaperone inhibition by the prion curing agent guanidinium chloride. J Biol Chem. 2013 Mar
940 8;288(10):7065–76.

941 79. Kalia J, Swartz KJ. Elucidating the molecular basis of action of a classic drug: guanidine
942 compounds as inhibitors of voltage-gated potassium channels. Mol Pharmacol. 2011
943 Dec;80(6):1085–95.

944 80. Sadeghipour S, Bek EJ, McMinn PC. Selection and characterisation of guanidine-resistant mutants
945 of human enterovirus 71. Virus Res. 2012 Oct;169(1):72–9.

946 81. Nelson JW, Atilho RM, Sherlock ME, Stockbridge RB, Breaker RR. Metabolism of Free Guanidine
947 in Bacteria Is Regulated by a Widespread Riboswitch Class. Mol Cell. 2017 Jan 19;65(2):220–30.

948 82. Williams DM, Wang D, Cole PA. Chemical rescue of a mutant protein-tyrosine kinase. J Biol Chem.
949 2000 Dec 8;275(49):38127–30.

950 83. Qiao Y, Molina H, Pandey A, Zhang J, Cole PA. Chemical rescue of a mutant enzyme in living cells.
951 Science. 2006 Mar 3;311(5765):1293–7.

952 84. Jones GW, Song Y, Masison DC. Deletion of the Hsp70 chaperone gene SSB causes
953 hypersensitivity to guanidine toxicity and curing of the [PSI+] prion by increasing guanidine
954 uptake in yeast. Mol Genet Genomics MGG. 2003 Jun;269(3):304–11.

955 85. Oh SJ, Kim DS, Head TC, Claussen GC. Low-dose guanidine and pyridostigmine: relatively safe and
956 effective long-term symptomatic therapy in Lambert-Eaton myasthenic syndrome. Muscle Nerve.
957 1997 Sep;20(9):1146–52.

958 86. Conn PM, Smithson DC, Hodder PS, Stewart MD, Behringer RR, Smith E, et al. Transitioning
959 pharmacoperones to therapeutic use: in vivo proof-of-principle and design of high throughput
960 screens. Pharmacol Res. 2014 May;83:38–51.

961 87. Kermani AA, Macdonald CB, Gundepudi R, Stockbridge RB. Guanidinium export is the primal
962 function of SMR family transporters. Proc Natl Acad Sci U S A. 2018 20;115(12):3060–5.

963 88. Bandyopadhyay A, Saxena K, Kasturia N, Dalal V, Bhatt N, Rajkumar A, et al. Chemical chaperones
964 assist intracellular folding to buffer mutational variations. Nat Chem Biol. 2012 Jan 15;8(3):238–
965 45.

966 89. Lindquist S. Protein folding sculpting evolutionary change. Cold Spring Harb Symp Quant Biol.
967 2009;74:103–8.

968 90. Amberg D, Burke D, Strathern J. Methods in Yeast Genetics: A Cold Spring Harbor Laboratory
969 Course Manual, 2005 Edition. Cold Spring Harbor Laboratory Press; 2005.

970 91. Akhmetov A, Laurent JM, Gollihar J, Gardner EC, Garge RK, Ellington AD, et al. Single-step
971 Precision Genome Editing in Yeast Using CRISPR-Cas9. Bio-Protoc. 2018 Mar 20;8(6).

972 92. Schaefer RM, Heasley LR, Odde DJ, McMurray MA. Kinetic partitioning during de novo septin
973 filament assembly creates a critical G1 "window of opportunity" for mutant septin function. Cell
974 Cycle Georget Tex. 2016 Jul 11;0.

975 93. Pringle JR, Preston RA, Adams AE, Stearns T, Drubin DG, Haarer BK, et al. Fluorescence
976 microscopy methods for yeast. Methods Cell Biol. 1989;31:357–435.

977 94. Bertin A, Nogales E. Characterization of Septin Ultrastructure in Budding Yeast Using Electron
978 Tomography. Methods Mol Biol Clifton NJ. 2016;1369:113–23.

979 95. Zhang Y. I-TASSER server for protein 3D structure prediction. BMC Bioinformatics. 2008 Jan
980 23;9:40.

981 96. Trott O, Olson AJ. AutoDock Vina: improving the speed and accuracy of docking with a new
982 scoring function, efficient optimization, and multithreading. J Comput Chem. 2010 Jan
983 30;31(2):455–61.

984 97. Pettersen EF, Goddard TD, Huang CC, Couch GS, Greenblatt DM, Meng EC, et al. UCSF Chimera--a
985 visualization system for exploratory research and analysis. J Comput Chem. 2004
986 Oct;25(13):1605–12.

987 98. Saccharomyces Genome Database [Internet]. Available from: www.yeastgenome.org

988 99. Ho J, Tumkaya T, Aryal S, Choi H, Claridge-Chang A. Moving beyond P values: data analysis with
989 estimation graphics. Nat Methods. 2019;16(7):565–6.

990 100. Brachmann CB, Davies A, Cost GJ, Caputo E, Li J, Hieter P, et al. Designer deletion strains derived
991 from Saccharomyces cerevisiae S288C: a useful set of strains and plasmids for PCR-mediated
992 gene disruption and other applications. Yeast. 1998 Jan 30;14(2):115–32.

993 101. Li Z, Vizeacoumar FJ, Bahr S, Li J, Warringer J, Vizeacoumar FS, et al. Systematic exploration of
994 essential yeast gene function with temperature-sensitive mutants. Nat Biotechnol. 2011
995 Apr;29(4):361–7.

996 102. McMurray MA, Thorner J. Septin stability and recycling during dynamic structural transitions in
997 cell division and development. Curr Biol CB. 2008 Aug 26;18(16):1203–8.

998 103. Winzeler EA, Shoemaker DD, Astromoff A, Liang H, Anderson K, Andre B, et al. Functional
999 Characterization of the S. cerevisiae Genome by Gene Deletion and Parallel Analysis. Science.
1000 1999 Aug 6;285(5429):901–6.

1001
1002

1003 **Figure 1. GdnHCl rescues the temperature-sensitive defects of *cdc10(D182N)* mutants in a**
1004 **manner that does not require Hsp104 or Hsp78.**
1005 (A) Dilution series of yeast cells spotted on rich (YPD) agar medium with or without 3 mM GdnHCl
1006 and incubated at the indicated temperatures for 3 days before imaging. Strains were: BY4741,
1007 CBY07236, CBY06417, CBY08756, and CBY05110.
1008 (B) As in (A), but only at 37°C and with strains of the indicated genotypes.
1009 (C) Amino acid alignment of regions *S. cerevisiae* Hsp104 and Hsp78 with *Thermus thermophilus*
1010 ClpB, showing conservation of residues (in red) that contact Gdm in the ClpB crystal structure (PDB
1011 4HSE).
1012 (D) As in (A), but at 37°C and with BY4741 ("WT") or CBY06417 ("*cdc10(D182N)*") cells and the
1013 indicated concentrations of GdnHCl. The cells were streaked with a toothpick, rather than spotted
1014 from dilutions. (E) Growth curves for the *cdc10(D182N)* strain CBY06417 at 37°C in the indicated
1015 concentrations of GdnHCl. The optical density at 600 nm ("OD_{600}") was measured at 5-min
1016 intervals. Each line shows the mean for 12 replicate cultures in the same row of the 96-well plate.
1017 Duplicate rows were monitored for each GdnHCl concentration.
1018
1019 **Figure 2. GdnHCl promotes exclusion of mutant Cdc10 molecules from higher-order septin**
1020 **assemblies.**
1021 (A) As in Figure 1B, but with the addition of *cdc10Δ* cells, and the cells were streaked with a
1022 toothpick, rather than spotted from dilutions.
1023 (B) Cultures of the strains JTY3985 ("*CDC10-GFP*") or JTY3986 ("*cdc10(D182N)-GFP*") were grown
1024 overnight in liquid culture at the indicated temperatures with or without 3 mM GdnHCl and then
1025 imaged by microscopy with transmitted light (left images) or for GFP fluorescence (right images).
1026 Fluorescence images were inverted to improve visibility.
1027 (C) Cells of the strain JTY4020 were cultured at 37°C with or without 5 mM GdnHCl and imaged as
1028 in (B), then linescans of bud neck fluorescence were performed for the indicated numbers of cells
1029 to quantify levels of Cdc10-mCherry (purple) or Cdc10(D182N)-GFP (green). For each data point,
1030 cytosolic signal was subtracted from bud neck signal; negative values thus indicate cytosolic signal
1031 greater than septin ring signal. In violin plots, solid lines indicate quartiles and dashed lines are
1032 medians.
1033 (D) In strain JTY5104, the chromosomal sources of Cdc3 and Cdc10 are eliminated by deletion and
1034 Cdc3(W364A) and Cdc10 are supplied by *LYS2*- or *URA3*-marked plasmids, respectively. Following

1035 introduction of *LEU2*-marked plasmid encoding WT Cdc3 (pFM831) or Cdc3-GFP (pML109), the
1036 transformants were passaged on medium with α-aminoadipate to select for loss of the
1037 *CDC3(W364A)* plasmid. These clones were then streaked, along with cells of the original strain
1038 JTY5104 carrying both plasmids ("*cdc10Δ CDC3(W364A)*"), on medium with 3 mM GdnHCl and 5-
1039 fluoro-orotic acid (FOA, to select for loss of the *CDC10* plasmid) and incubated for 4 days at 22°C.
1040

1041 **Figure 3. GdnHCl promotes higher-order assembly by recombinant Cdc10-less septin**
1042 **hexamers produced heterologously in *E. coli*.**
1043 (A) SDS-PAGE and Coomassie staining of septin complexes purified from *E. coli* cells co-
1044 expressing Cdc3, Cdc11, and 6xHis-Cdc12 in high-salt buffer to prevent filament polymerization
1045 were diluted into low salt to allow polymerization, then filaments were pelleted by centrifugation.
1046 Equal amounts of samples prepared with or without 100 mM GdnHCl present during expression
1047 and throughout all subsequent steps were loaded. Band intensities for the low-salt pellet and
1048 supernatant ("Sup") fractions were determined by linescans of the gel image and are plotted to the
1049 right, color-coded with the labels above the gel lanes. At left, molecular weight markers.
1050 (B) As in (A), but GdnHCl was added only after cell lysis. (C) Immunoblot for Cdc11 using one of
1051 the samples shown in (A).
1052

1053 **Figure 4. Parallel *in silico* modeling and phylogenetic analysis independently point to Gdm**
1054 **binding near Thr302 and His262 in Cdc3.**
1055 (A) A model of the structure of Cdc3 based on SEPT2•GppNHp (PDB 3FTQ) was used for unbiased
1056 *in silico* docking of Gdm. The top 5 predicted sites of Gdm binding are shown (red), labeled with
1057 predicted free energies of binding, in kcal/mol. Thr302 is in blue, His262 in orange. "α4", α4 helix;
1058 "*t*L1", *trans* loop 1.
1059 (B) Cartoon ribbon view of human septin G homodimer crystal structures showing selected
1060 sidechains. Red, residues corresponding to the non-conservative changes seen in the phylogenetic
1061 analysis in S2 Fig. Blue, conserved His residue of *trans* loop 1 and Asp residue of Switch II region.
1062 Orange, GTP analog. Red asterisk, Arg in α4 helix. "α4", α4 helix; "*t*L1", *trans* loop 1; "Sw1", Switch
1063 I; "Sw2", Switch II; "G1", G1 motif/P-loop.
1064

1065 **Figure 5. GdnHCl rescues *cdc10Δ* in *A. gossypii.***
1066 *AgSHS1-GFP Agcdc10Δ* strain AG135 was grown with shaking for 15 hours at 37°C in complete

1067 (AFM) medium, after which the culture was split in two and GdnHCl was added to one aliquot to
1068 30 mM final concentration. Cells were imaged after an additional 3 hours growth with shaking.
1069 Purple rectangles indicate the approximate region enlarged at right ("Zoom"). Scale bar, 10 µm.
1070
1071 **Figure 6. Partial rescue of TS defects by GdnHCl derivatives.**
1072 (A) WT strain BY4741 was cultured overnight in rich (YPD) medium containing the indicated
1073 concentrations of urea, and the density of each culture was determined with a spectrophotometer.
1074 (B) BY4741 ("WT") or the *cdc10(D182N)* strain CBY06417 ("*cdc10*") were streaked on plates
1075 containing no or 0.64 M urea and incubated at the indicated temperature for 3 days before imaging.
1076 (C) Cells from saturated YPD cultures of strains used in (A) were plated to form a monolayer on the
1077 surface of a rich (YPD) agar plate, and a 1-cm-diameter filter disk spotted with 5 *µ*L of the indicated
1078 drug was placed in the center of the plate. The plate was imaged after incubation at 37ºC for 3 days.
1079 (D) As in Fig 1A, for strains of the indicated genotypes grown on medium containing 0 or 0.375 mM
1080 of each indicated drug.
1081 (E) As in Fig 4A, but zoomed into the area between Thr302 and His262, and including the Gdm
1082 derivatives aminoguanidine ("aGdm") and N-ethylguanidine ("eGdm").
1083 (F) As in (B), but with the addition of strain CBY06420 ("*cdc10(G100E)*") and with arginine
1084 hydrochloride instead of urea.
1085
1086 **Figure 7. Arg at position 302 in Cdc3 blocks rescue of *cdc10* by GdnHCl.**
1087 As in Fig 2D, strain JTY5104 was transformed with a plasmid encoding GFP-tagged Cdc3 (pML109)
1088 or derivatives in which the residue at position 302 was mutated from Thr to Val or Arg, followed by
1089 selection for loss of the plasmids encoding wild-type Cdc3 and Cdc10. Serial dilutions of the
1090 resulting strains were spotted on rich (YPD) medium at the indicated temperatures and containing
1091 GdnHCl where indicated, and imaged after 3 days.
1092
1093 **Figure 8. Reversing evolution to reactivate Cdc3 GTPase activity allows Cdc10 bypass**
1094 **during septin hetero-oligomerization.**
1095 (A) Strain MMY0130, which carries the mutations *cdc3(D210G) cdc10(D182N)*, was transformed
1096 with plasmid YCpK-Cdc10-1-GFP and cultured in rich (YPD) medium containing G-418 for plasmid
1097 selection in the presence or absence of GdnHCl. Bud neck fluorescence was measured as in Fig
1098 2B.

1099 (B) Haploid strains of the indicated genotypes expressing Cdc10-mCherry and Shs1-GFP were
1100 imaged as in (A) but in the absence of GdnHCl and for both mCherry and GFP fluorescence. For
1101 each cell, the ratio of mCherry to GFP signal was calculated; values are plotted on the left axis, with
1102 overlaid blue violin plots to show how the data are distributed, and median (dashed lines) and
1103 quartiles (solid lines) shown in green. The right axis shows the median difference ("effect size") for
1104 comparisons of the mutant strains against the shared wild-type control, plotted as bootstrap
1105 sampling distributions (gray violin plots). Each median difference is depicted as a block dot, with the
1106 value of that difference given in gray. Each 95% confidence interval is indicated by the ends of the
1107 vertical error bars. Strains were: MMY0342, MMY0343, and MMY0350.
1108 (C) Serial dilutions of the strains in (B) were spotted on rich (YPD) agar media with or without
1109 GdnHCl and incubated for 4 days at the indicated temperatures.
1110 (D) A portion of the *CDC10* coding sequence was amplified by PCR and sequenced. Asterisk in the
1111 chromatograph at left shows the mutation resulting in the amino acid change Q265H. Right,
1112 alignment of septin sequences surrounding the conserved Trp (bold) of the Sep4 motif and the His
1113 (bold) with which this Trp interacts across the G interface, as illustrated in (E). Red, Gln265 in wild-
1114 type Cdc10.
1115 (E) The Trp and His residues of the Sep4 motif in the SEPT2•GppNHp homodimer crystal structure
1116 (PDB 3FTQ).
1117
1118 **S1 Figure. GdnHCl rescues high-temperature septin function and neck filament assembly in**
1119 ***cdc10* mutants, related to Fig 1.**
1120 (A) Dilution series of cells of the indicated genotypes (strains BY4741, CBY06417, CBY06420, or
1121 CBY06424) spotted on YPD plates with or without 3 mM GdnHCl and incubated at 37° C.
1122 (B) anti-Cdc11 antibodies were used to stain *cdc10Δ* cells cultured at 37° C. Arrowhead, septin ring.
1123 (C) Cells of the *cdc10(D182N)-GFP* strain JTY3986 were cultured at 37° C in liquid YPD with 3 mM
1124 GdnHCl, cryo-fixed, cryo-substituted, sectioned, and stained with uranyl acetate prior to imaging by
1125 EM. Arrowheads indicate neck filaments tightly apposed to the plasma membrane.
1126
1127 **S2 Figure. Co-variation during evolution of Cdc3 residues clustered around the *trans* loop 1**
1128 **of the G dimerization interface identifies an Arg residue "missing" in species that poorly**
1129 **tolerate *cdc10Δ*, related to Fig 4.**
1130 Amino acid alignment of sequences of Cdc3 and its homologs in fungal species for which the

1131 phenotypic consequences of deletion or mutation of *CDC10* have been characterized in relation to
1132 deletion or mutation of *CDC3*. Names of species and the protein homologous to Cdc3 are color-
1133 coded: blue, species for which mutation of the *CDC10* homolog is as severe as mutation of the
1134 *CDC3* homolog; orange, species for which mutation of *CDC10* is clearly less severe than mutation
1135 of the *CDC3* homolog. Non-CTE human septin sequences are shown below for comparison with
1136 crystal structures of those septins shown in Fig 4B. Shading or boxing indicates residues that are
1137 either the same in *S. cerevisiae*, *A. gossypii*, and *K. lactis* and something different in the other fungal
1138 species, and/or the same in the other species and something different in *S. cerevisiae*, *A. gossypii*,
1139 and *K. lactis*. Gray, conservative changes; red, non-conservative changes. Red box: position 302
1140 in ScCdc3. Key structural features are indicated above each group of sequences; "α0", α0 helix;
1141 "α4", a4 helix; "Sw I", Switch I loop; "G4", G4 motif. Sc, *S. cerevisiae* (KZV09558); Ag, *A. gossypii*
1142 (NP_985658); Kl, *K. lactis* (CAH00343), Ca, *C. albicans* (EEQ42751); An, *A. nidulans* (AAB41233);
1143 Cn, *C. neoformans* (XP_012050631); Fg, *F. graminearum* (ESU11253); Nc, *N. crassa* (ESA42882);
1144 Sp, *S. pombe* (CAB11714); Um, *U. maydis* (KIS68154); Mo, *M. oryzae* (ELQ45022); Cc, *C. cinerea*
1145 (XP_001828599); HsSEPT2, *H. sapiens* SEPT2 (AAH33559); HsSEPT9, *H. sapiens* SEPT9
1146 (AAH54004).
1147
1148 **S3 Figure. Sequence of the Cdc3-AspB chimeric protein and comparison of key residues**
1149 **between Cdc3, AspB, and Cdc12, related to Fig 8.**
1150 Alignments of *S. cerevisiae* Cdc3 with *Aspergillus nidulans* AspB and the Cdc3-AspB chimera
1151 (above), and with *S. cerevisiae* Cdc12 and *A. nidulans* AspB (below). Red highlighting indicates
1152 positions that covary with the catalytic Thr in Cdc3 homologs, as in S2 Fig.
1153
1154 **S4 Figure. Five substitutions in the GTPase domain of Cdc3 are insufficient to promote**
1155 **bypass of Cdc10 during septin assembly, related to Fig 8.**
1156 Strains of the indicated genotypes (JTY5397, MMY0361, MMY0362 and MMY0363) were grown to
1157 mid-logarithmic phase in liquid rich (YPD) medium and levels of Shs1-GFP and Cdc10-mCherry
1158 within septin rings were measured as in Fig 8B, and plotted in (A) with effect size (median difference)
1159 distributions plotted in (B).
1160
1161 **S5 Figure. Contacts between α4 Arg and *trans* loop 1 are conserved in the distant septin**
1162 **relative Toc34, related to Fig 4.**

1163 (A) Structures of homodimer interface of Toc34 from *Arabidopsis thaliana*i (GppNHp-bound, PDB
1164 3bb3, top) and *Pisum sativum* (GDP-bound, PDB 1h65, bottom) with nucleotide in orange, α4 Arg
1165 in red and nucleotide-contacting *trans* loop 1 ("TL1") residues in blue.
1166 (B) Sequence alignment of a region in and around the α4 helix of Toc34 homologs in various plant
1167 species, with identical and variable amino acids in black and red, respectively, and the α4 Arg in
1168 bold. *A. thaliania*, At (NP_196119); *A. lyrata*, Al (XP_002873181); *Camelina sativa*, Cs
1169 (XP_010423506); *Brassica napus*, Bn (CDX98810); *Noccaea caerulescens*, Nc (JAU73517); *B.*
1170 *rapa*, Br (XP_009130855); *Eutrema salsugineum*, Es (XP_006398957); *Vitis vinifera*, Vv
1171 (XP_002274573); *Eucalyptus grandis*, Eg (XP_010063039); *P. sativum*, Ps (Q41009); *Nicotiana*
1172 *tabacum*, Nt (XP_016456518); *Zea mays*, Zm (ACG34570).
1173
1174 **S6 Figure. Rapid drift of Cdc3 α4 Thr in species of the genus *Saccharomyces* and strict**
1175 **conservation of α4 Arg in *Candida* species, related to Fig 4.**
1176 Sequence alignments of a region surrounding ScCdc3 Thr302 (highlighted in yellow), with identical
1177 and variable amino acids in black and red, respectively. Percent sequence identity over the entirety
1178 of Cdc3, relative to ScCdc3 or CaCdc3, is given at left. Alignments of *Saccharomyces* species were
1179 performed using the Saccharomyces Genome Database (http://www.yeastgenome.org). Sc, *S.*
1180 *cerevisiae*; Sp, *S. paradoxus*; Sm, *S. mikatae*; Sa, *S. aboricola*; Sb, *S. bayanus*; Su, *S. uvarum*; Sk,
1181 *S. kudriavzevii*. *Candida* alignments were performed at the NCBI Blast server. Ca, *C. albicans*
1182 (EEQ42751); Cd, *C. dubliniensis* (CAX44656); Cm, *C. maltosa* (EMG46918); Cr, *C. tropicalis*
1183 (XP_002550438); Ct, *C. tenuis* (EGV60285); Cg, *C. glabrata* (CAG57768).
1184
1185 **S7 Figure. Model for the roles of key molecular features during the evolution of septin**
1186 **complexes, related to Fig 8.**
1187 (A) A model of the evolution of septin hetero-octamers in *S. cerevisiae* from an ancestral homo-
1188 oligomer. Stars indicate the number of phosphate groups on bound nucleotide. Abbreviations:
1189 "CTE", carboxy-terminal extension; "α4", Arg and Asp residues of the α4 helix; "Sw2", Switch II
1190 region; "*t*L1", trans loop 1".
1191 (B) Illustration of the "revised" order of septin subunits in human hetero-octamers and hetero-
1192 hexamers, including the predicted phosphorylation state of bound nucleotides, as indicated by the
1193 number of black stars. SEPT9 is given as an example SEPT3-group subunit.
1194

S1 Table

Fungal strains used in this study.

Name* (species)	***Relevant genotype***	***Source/Reference***
(S.c.)[a]	*cdc10(D182N)-GFP::URA3 hsp78Δ::kanMX*	This study
(S.c.)[a]	*cdc10(D182N)-GFP::URA3 hsp104Δ::kanMX*	This study
(S.c.)[a]	*cdc10(D182N)-GFP::URA3 hsp78Δ::kanMX hsp104Δ::kanMX*	This study
Ag135 (A.g., also called AgHPH14)	*cdc10Δ::GEN1 SHS1-GFP–NAT1*	(54)
BY4741 (S.c.)	*MAT**a** his3Δ1 leu2Δ0 ura3Δ0 met15Δ0*	(100)
BY4742 (S.c.)	*MATα his3Δ1 leu2Δ0 ura3Δ0 lys2Δ0*	(100)
CBY05110 (S.c.)	BY4741 "*cdc12-1" cdc12(G247E)::KanMX*	(101)
CBY06417 (S.c.)	BY4741 "*cdc10-1" cdc10(D182N)::KanMX*	(101)
CBY06420 (S.c.)	BY4741 "*cdc10-2" cdc10(G100E)::KanMX*	(101)
CBY06424 (S.c.)	BY4741 "*cdc10-5" cdc10(G44D)::KanMX*	(101)
CBY06427 (S.c.)	BY4741 *cdc11(G29D)::KanMX*	(101)
CBY07236 (S.c.)	BY4741 *"cdc3-3" cdc3(G365R)::KanMX*	(101)
CBY08756 (S.c.)	BY4741 "*cdc11-1" cdc11(G32E I142T)::KanMX*	(101)
JTY3985 (S.c.)	BY4741 *CDC10-GFP::URA3*	(30)
JTY3986 (S.c.)	BY4741 *cdc10(D182N)-GFP::URA3*	(30)
JTY3992 (S.c.)	BY4741 *CDC10-mCherry::KanMX*	(102)
JTY3993 (S.c.)	BY4742 *CDC10-mCherry::KanMX*	(102)
JTY4013 (S.c.)	BY4742 *hsp104Δ::kanMX*	(103)
JTY4014 (S.c.)	BY4741 *hsp104Δ::KanMX*	(103)
JTY4020[b] (S.c.)	BY4743 *CDC10-mCherry::kanMX/cdc10(D182N)-*	This study
JTY4203 (S.c.)	*cdc10Δ::kanMX* [*CDC10 URA3*]	(23)
JTY5104 (S.c.)	*cdc3Δ cdc10Δ* [*CDC3(W364A) LYS2*] [*CDC10 URA3*]	(23)
JTY5397 (S.c.)	BY4741 *CDC10-mCherry::kanMX SHS1-GFP::HIS3MX6*	(58)
MMY0110 (S.c.)	*cdc3(D210G) cdc10(D182N)*	(29)
MMY0130 (S.c.)	*cdc3(D210G) cdc10(D182N)*	(29)
MMY0131 (S.c.)	*cdc3(D210G)*	(29)
(S.c.)	BY4742 *hsp78Δ::kanMX*	(103)
(S.c.)	BY4742 *hsp104Δ::KanMX*	(103)

MMY0343[c]	BY4741 *CDC10-mCherry::kanMX SHS1-GFP::HIS3MX6 cdc3(95-341)::aspB(6-234)*	This study
MMY0350[c]	BY4741 *cdc10(Q265H)-mCherry::kanMX SHS1-GFP::HIS3MX6 cdc3::aspB(6-234)*	This study
MMY0361[c]	BY4741 *CDC10-mCherry::kanMX SHS1-GFP::HIS3MX6 CDC3(P127E D128S K181T T302R Q306D)*	This study
MMY0362[c]	BY4741 *CDC10-mCherry::kanMX SHS1-GFP::HIS3MX6 CDC3"recoded"*	This study
MMY0363[c]	BY4741 *CDC10-mCherry::kanMX SHS1-GFP::HIS3MX6 CDC3(T302R Q306D)*	This study

* Strains lacking names were generated by crossing other named strains or by selecting for loss of a plasmid from a named strain, and were used immediately thereafter. Their use in specific experiments in this study can be identified by their genotypes.

[a] Made by mating JTY3986 with the appropriate *hsp* deletion strain, or by mating of the *cdc10(D182N) hsp78Δ* strain with JTY4013, followed by sporulation and dissection of tetrads, then identification of genotypes via testing of marker phenotypes or segregation thereof (*e.g.* 2:2 segregation of G-418 resistance for *cdc10(D182N) hsp78Δ::kanMX hsp104Δ::kanMX*). Genotypes at other marker loci (*MAT*, *MET15*, *LYS2*, etc.) were not determined.

[b] Made by mating JTY3993 with JTY3985.

[c] Derived from JTY5397. See Methods section for details. Following confirmation of the integration via PCR and sequencing, spontaneous loss of plasmid pEM-CDC3-CRISPR1 was selected using 5-FOA.

1208 **S2 Table. Oligonucleotides used in this study.**

Name	Sequence (5’ -> 3’)
Cdc3AspBfw	GGTATGGGCATCACCTCCTCTCAGAGCGAAAAGG GTCAAGTTCTGCCTGACCAACCGGAGATTAAGTTC ATTCGCCGGAAGCTAACCGGC
Cdc3AspBextend1	GGAACGGCCTCTCACTTGATTACCGCTATAATTTT CCACGATGTCGTTGGAACCAATAACGGCAAAAGG AACCTTCGACAT
Cdc3GTPase_extend2	TTTCAAAAGGTTGAAATCAGAGTGGTTGTCATTGT CCACTTCGATCACCCCCCATGGATAGGAACGGCC TCTCACTTG
5’cdc3fw	AACTGAACGATTACATCGGC
3’cdc3re	TGTTTGAAATTTTTATATGTC
5’cdc10fw	CACGGTTACTACAAGCACTCT
3’cdc10re	TCACCACCATTCTTATGAGA
cdc10midfw	CCAAATGGAAAGGAGTTGAGC
CDC3GTPaserecode	ATTCGTCGTCAAATCAATGGTTATGTAGGGTTTGC TAATTTGCCCAAGCAATGGCACAGAAGGTCCATAA AGAACGGATTCAGTTTCAATCTCCTATGTGTCGGC GAGAGCGGTATAGGTAAGACAACATTAATGAAAAC ATTATTTAATAACGATGATATTGAAGCCAATTTAGT CAAAGATTACGAAGAGGAACTTGCTAATGATCAGG AGGAAGAGGAGGGACAGGGCGAGGGACACGAGA ACCAGTCACAAGAGCAAAGGCACACTGTCAAAAT CAAGTCATATGAGTCGGTTATTGAAGAAAATGGTG TTAAACTGAATTTGAACGTGATCGATACTGAAGGA TTTGGTGATTTTTTAAATAATGATCAAAAATCATGG GACCCGATCATTAAGGAGATTGACTCACGTTTTGA CCAATACTTAGATGCGGAGAATAAAATCAATAGAC ATTCTATAAACGACAAAAGAATCCACGCATGTCTA TATTTCATTGAGCCTACAGGACACTACTTAAAGCC GCTGGACCTTAAGTTTATGCAGTCAGTATATGAGA AATGTAATTTGATTCCTGTAATTGCTAAATCAGACA TCTTAACAGATGAAGAGATATTATCCTTCAAGAAG AGAATTATGAACGATTTAATACAATCAAATATAGAG CTTTTCAAACCACCAATATACTCCAACGATGACGC CGAAAATAGCCACTTGTCCGAAAGACTATTTTCCT CCTTACCTTACGCAGTTATTGGTTCAAATGACATC GTGGAAAATTATAGCGGTAATCAAGTGAGAGGCC GTTCCTATCCATGGGGGGTGATCGAAGTGGACAA TGACAACCACTCTGATTTCAACCTTTTGAAA
CDC3recode	ATTCGTCGTCAAATCAATGGTTATGTAGGGTTTGC TAATTTGCCCAAGCAATGGCACAGAAGGTCCATAA AGAACGGATTCAGTTTCAATCTCCTATGTGTCGGC CCTGATGGTATAGGTAAGACAACATTAATGAAAAC ATTATTTAATAACGATGATATTGAAGCCAATTTAGT CAAAGATTACGAAGAGGAACTTGCTAATGATCAGG AGGAAGAGGAGGGACAGGGCGAGGGACACGAGA

	ACCAGTCACAAGAGCAAAGGCACAAGGTCAAAAT CAAGTCATATGAGTCGGTTATTGAAGAAAATGGTG TTAAACTGAATTTGAACGTGATCGATACTGAAGGA TTTGGTGATTTTTTAAATAATGATCAAAAATCATGG GACCCGATCATTAAGGAGATTGACTCACGTTTTGA CCAATACTTAGATGCGGAGAATAAAATCAATAGAC ATTCTATAAACGACAAAAGAATCCACGCATGTCTA TATTTCATTGAGCCTACAGGACACTACTTAAAGCC GCTGGACCTTAAGTTTATGCAGTCAGTATATGAGA AATGTAATTTGATTCCTGTAATTGCTAAATCAGACA TCTTAACAGATGAAGAGATATTATCCTTCAAGAAG ACCATTATGAACCAGTTAATACAATCAAATATAGA GCTTTTCAAACCACCAATATACTCCAACGATGACG CCGAAAATAGCCACTTGTCCGAAAGACTATTTTCC TCCTTACCTTACGCAGTTATTGGTTCAAATGACAT CGTGGAAAATTATAGCGGTAATCAAGTGAGAGGC CGTTCCTATCCATGGGGGGTGATCGAAGTGGACA ATGACAACCACTCTGATTTCAACCTTTTGAAA
G1KTTRQDfw	ATTCGTCGTCAAATCAATGGTTATG
Cdc3recodere	TTTCAAAAGGTTGAAATCAGAGTGG

1209

Figure 1

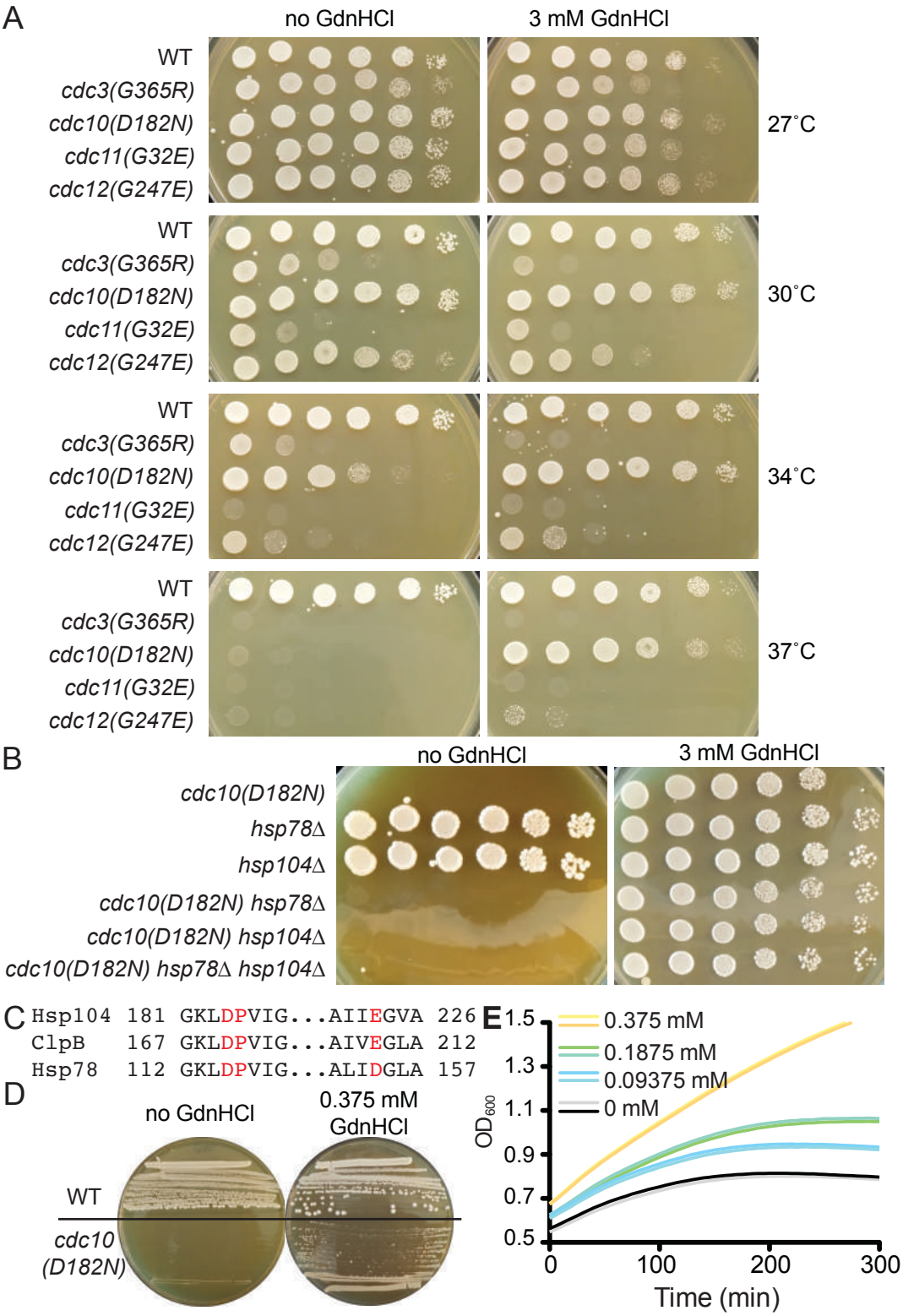
A
no GdnHCl
3 mM GdnHCl
WT
cdc3(G365R)
cdc10(D182N)
cdc11(G32E)
cdc12(G247E)
27˚C
30˚C
34˚C
37˚C
B
no GdnHCl
3 mM GdnHCl
cdc10(D182N)
hsp78Δ
hsp104Δ
cdc10(D182N) hsp78Δ
cdc10(D182N) hsp104Δ
cdc10(D182N) hsp78Δ hsp104Δ
C
Hsp104 181 GKLDPVIG...AIIEGVA 226
ClpB 167 GKLDPVIG...AIVEGLA 212
Hsp78 112 GKLDPVIG...ALIDGLA 157
D
no GdnHCl
0.375 mM GdnHCl
WT
cdc10 (D182N)
E
0.375 mM
0.1875 mM
0.09375 mM
0 mM
OD600
1.5
1.3
1.1
0.9
0.7
0.5
0
100
200
300
Time (min)

Figure 2

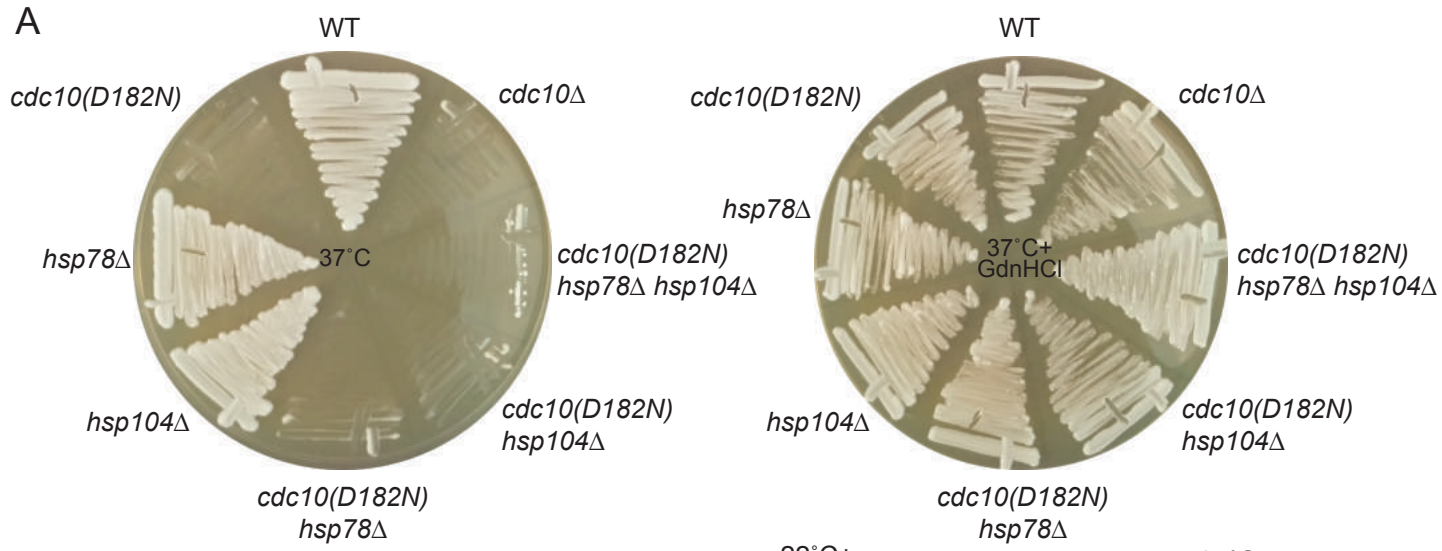
A
WT
cdc10(D182N)
cdc10Δ
hsp78Δ
37˚C
cdc10(D182N)
hsp78Δ hsp104Δ
hsp104Δ
cdc10(D182N)
hsp104Δ
cdc10(D182N)
hsp78Δ
WT
cdc10(D182N)
cdc10Δ
hsp78Δ
37˚C+
GdnHCl
cdc10(D182N)
hsp78Δ hsp104Δ
hsp104Δ
cdc10(D182N)
hsp104Δ
cdc10(D182N)
hsp78Δ

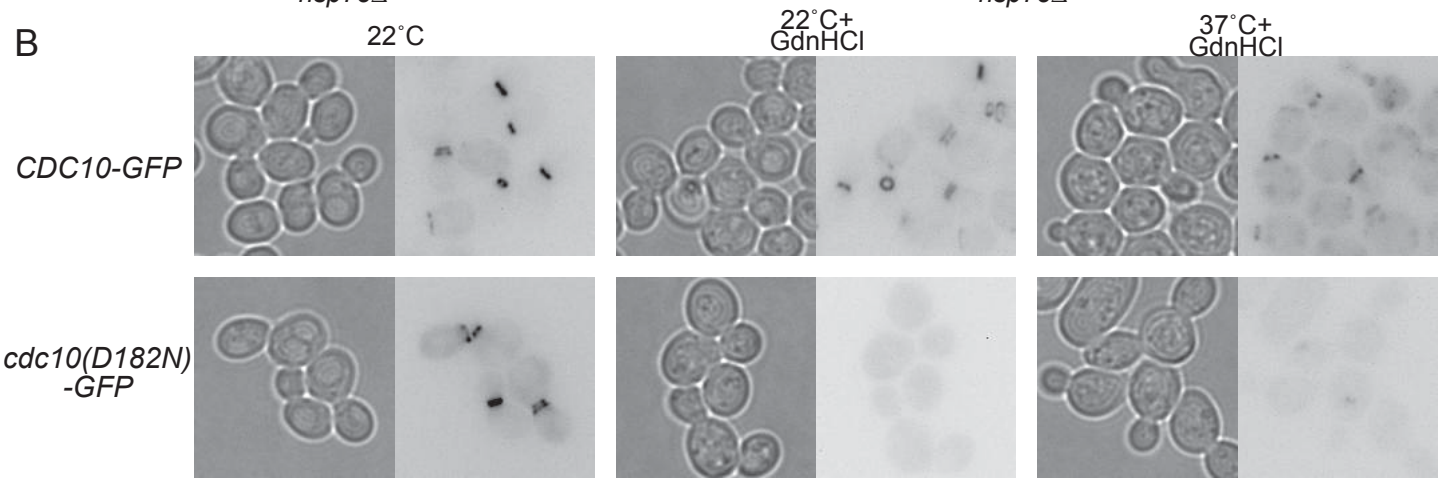
B
22˚C
22˚C+
GdnHCl
37˚C+
GdnHCl
CDC10-GFP
cdc10(D182N)
-GFP

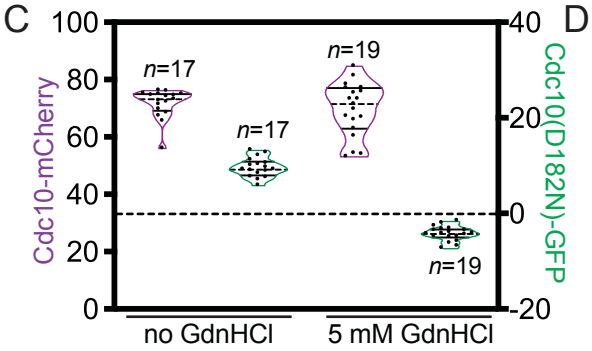
C
100
80
60
40
20
0
40
20
0
-20
Cdc10-mCherry
Cdc10(D182N)-GFP
n=17
n=17
n=19
n=19
no GdnHCl
5 mM GdnHCl

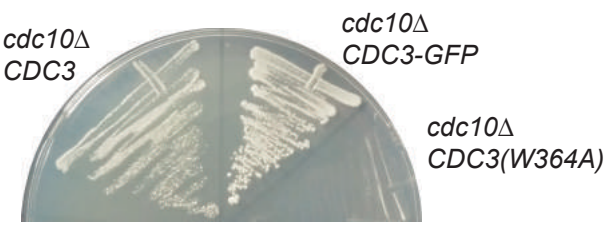
D
cdc10Δ
CDC3
cdc10Δ
CDC3-GFP
cdc10Δ
CDC3(W364A)

Figure 3

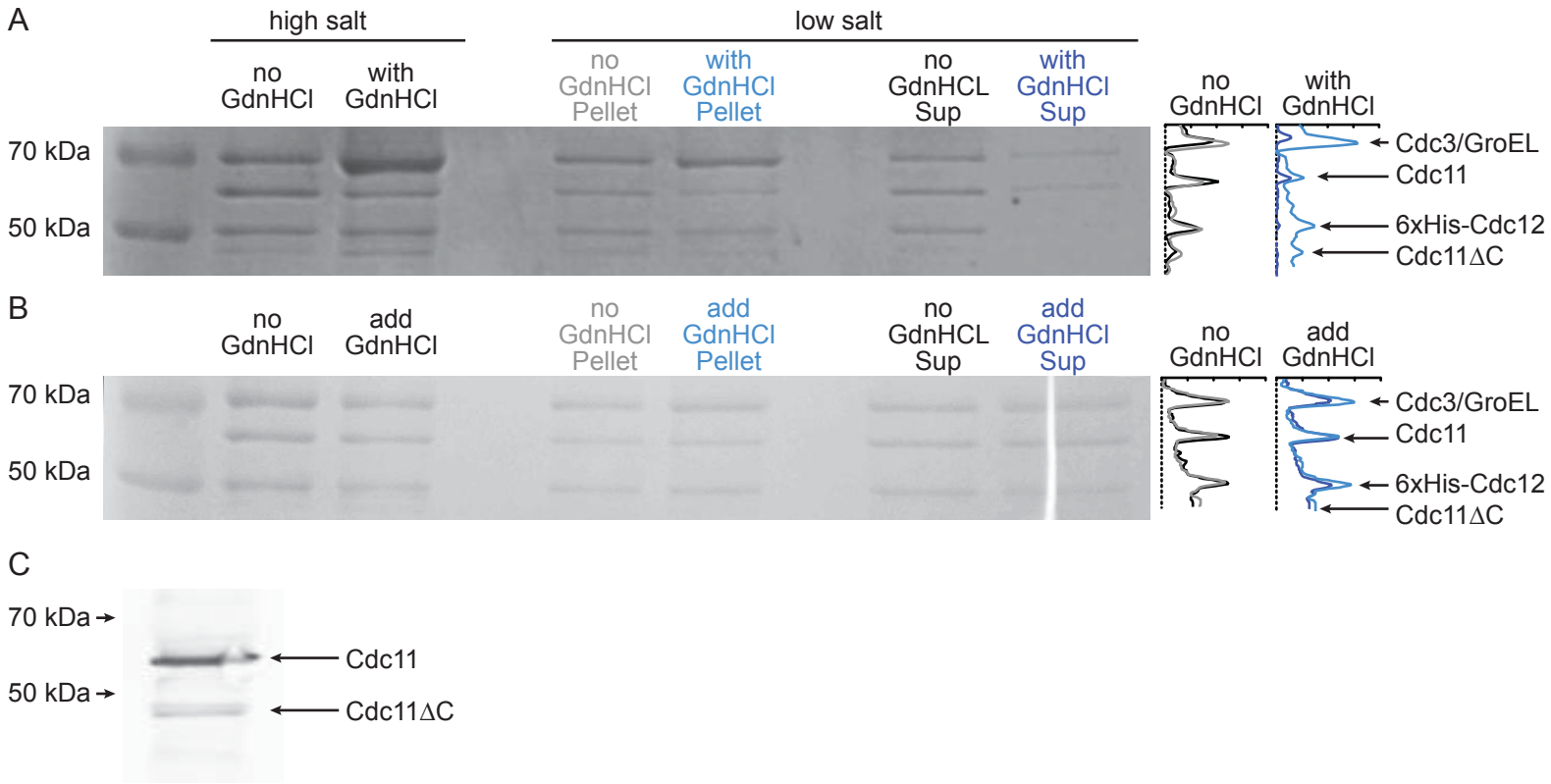
A
high salt
low salt
no GdnHCl
with GdnHCl
no GdnHCl Pellet
with GdnHCl Pellet
no GdnHCL Sup
with GdnHCl Sup
70 kDa
50 kDa
no GdnHCl
with GdnHCl
Cdc3/GroEL
Cdc11
6xHis-Cdc12
Cdc11ΔC
B
no GdnHCl
add GdnHCl
no GdnHCl Pellet
add GdnHCl Pellet
no GdnHCL Sup
add GdnHCl Sup
70 kDa
50 kDa
no GdnHCl
add GdnHCl
Cdc3/GroEL
Cdc11
6xHis-Cdc12
Cdc11ΔC

C
70 kDa
50 kDa
Cdc11
Cdc11ΔC

Figure 4

A

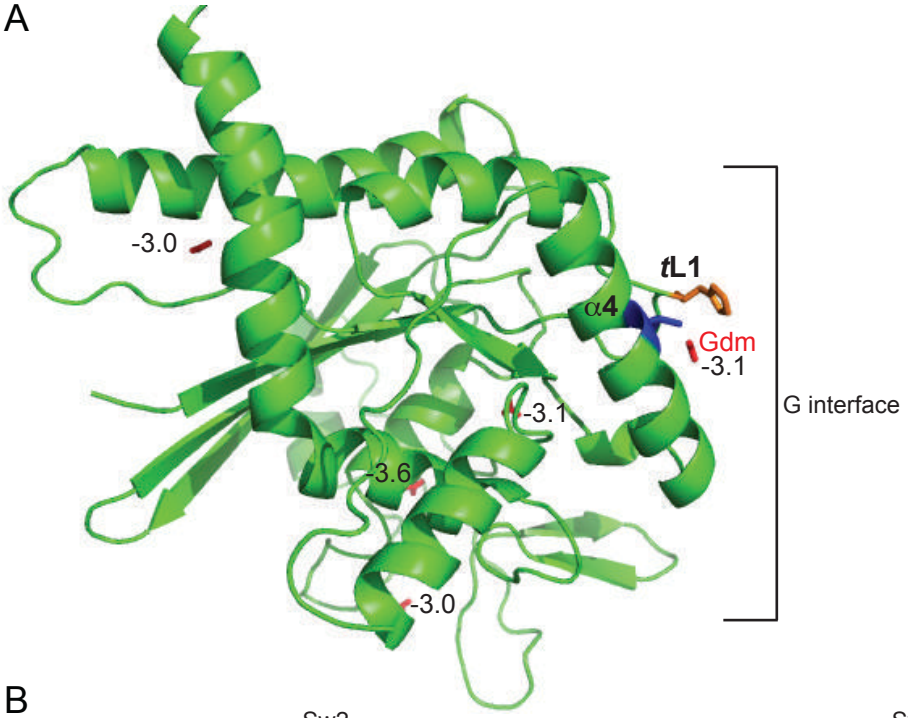

B

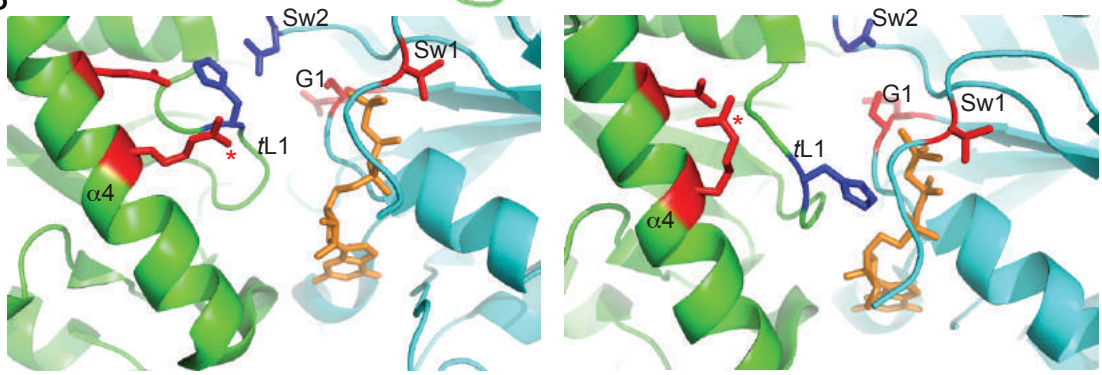

SEPT2•GppNHp

SEPT9•GTPγS

Figure 5

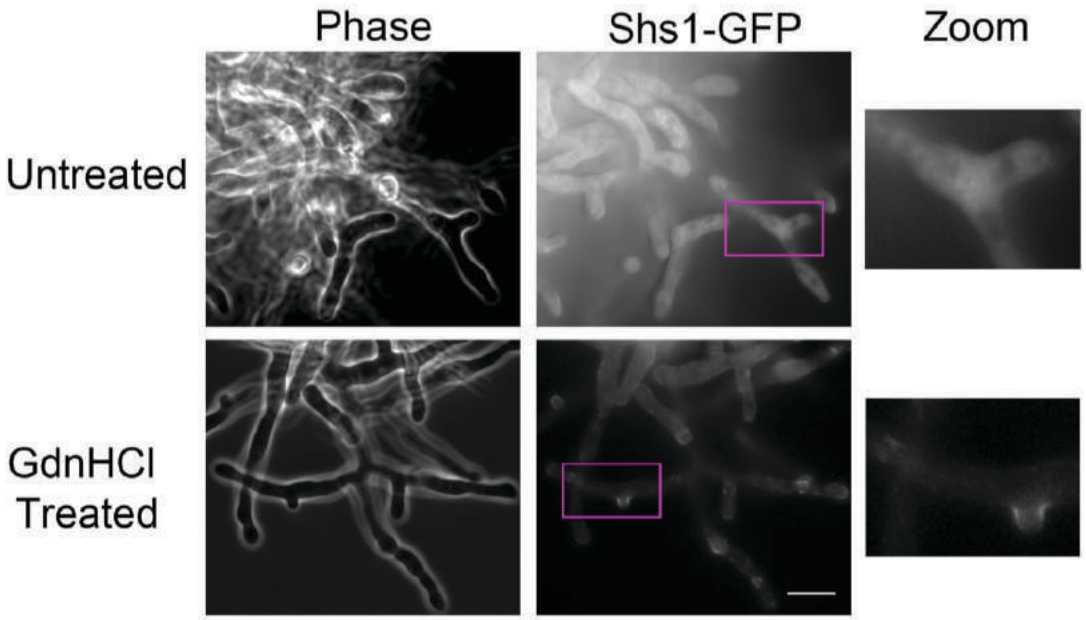

Figure 6

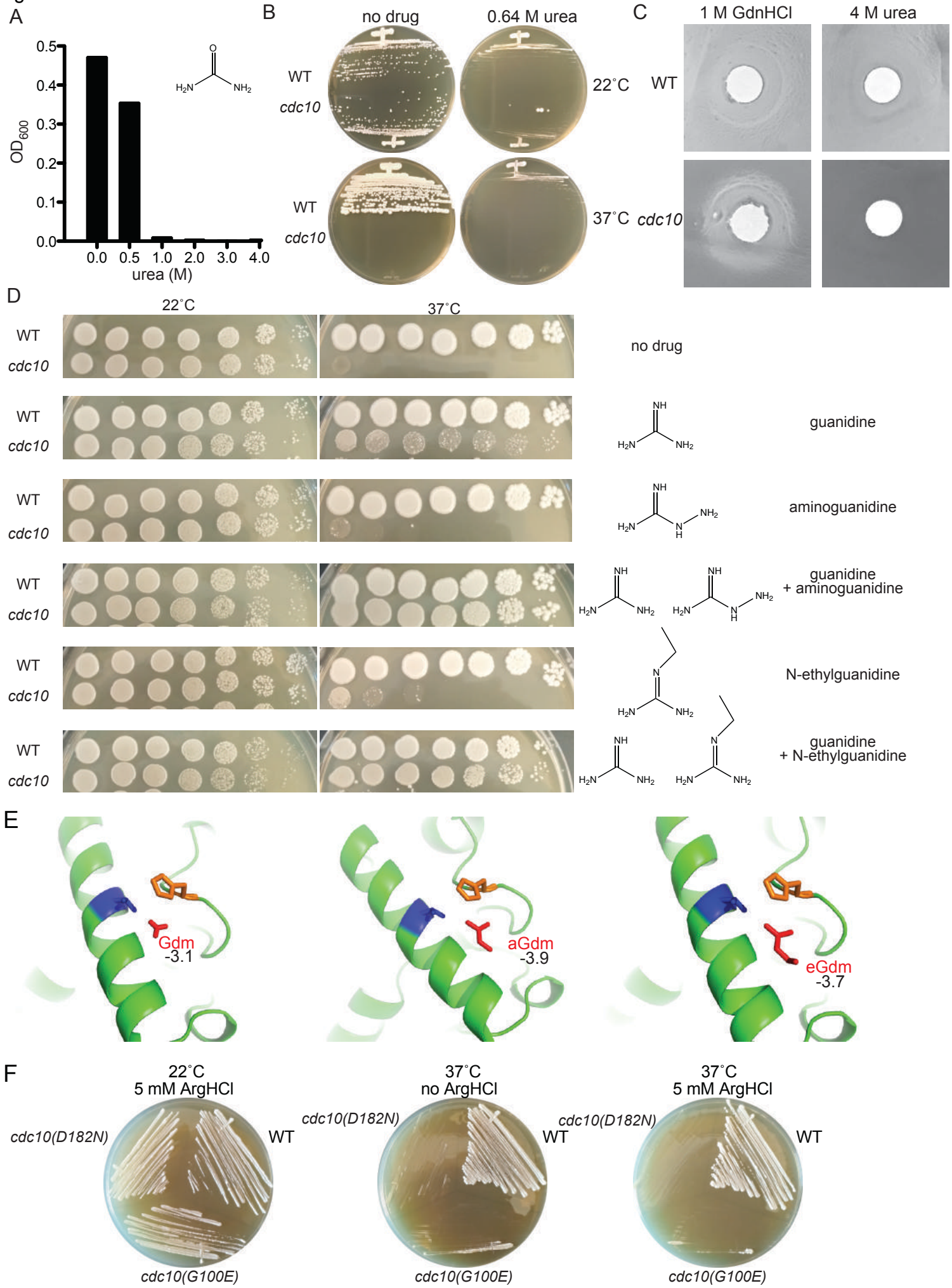
A
0.5
0.4
0.3
0.2
0.1
0.0
OD600
0.0 0.5 1.0 2.0 3.0 4.0
urea (M)
O
H2N NH2
B
no drug
0.64 M urea
WT
cdc10
22˚C
37˚C
C
1 M GdnHCl
4 M urea
WT
cdc10
D
22˚C
37˚C
WT
cdc10
no drug
guanidine
aminoguanidine
guanidine
+ aminoguanidine
N-ethylguanidine
guanidine
+ N-ethylguanidine
NH
H2N NH2
N
H
E
Gdm
-3.1
aGdm
-3.9
eGdm
-3.7
F
22˚C
5 mM ArgHCl
37˚C
no ArgHCl
37˚C
5 mM ArgHCl
cdc10(D182N)
WT
cdc10(G100E)

Figure 7

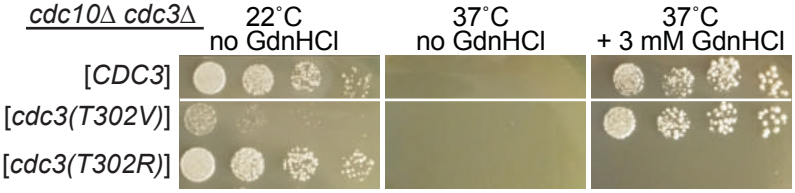
cdc10Δ cdc3Δ
22˚C
no GdnHCl
37˚C
no GdnHCl
37˚C
+ 3 mM GdnHCl
[CDC3]
[cdc3(T302V)]
[cdc3(T302R)]

Figure 8

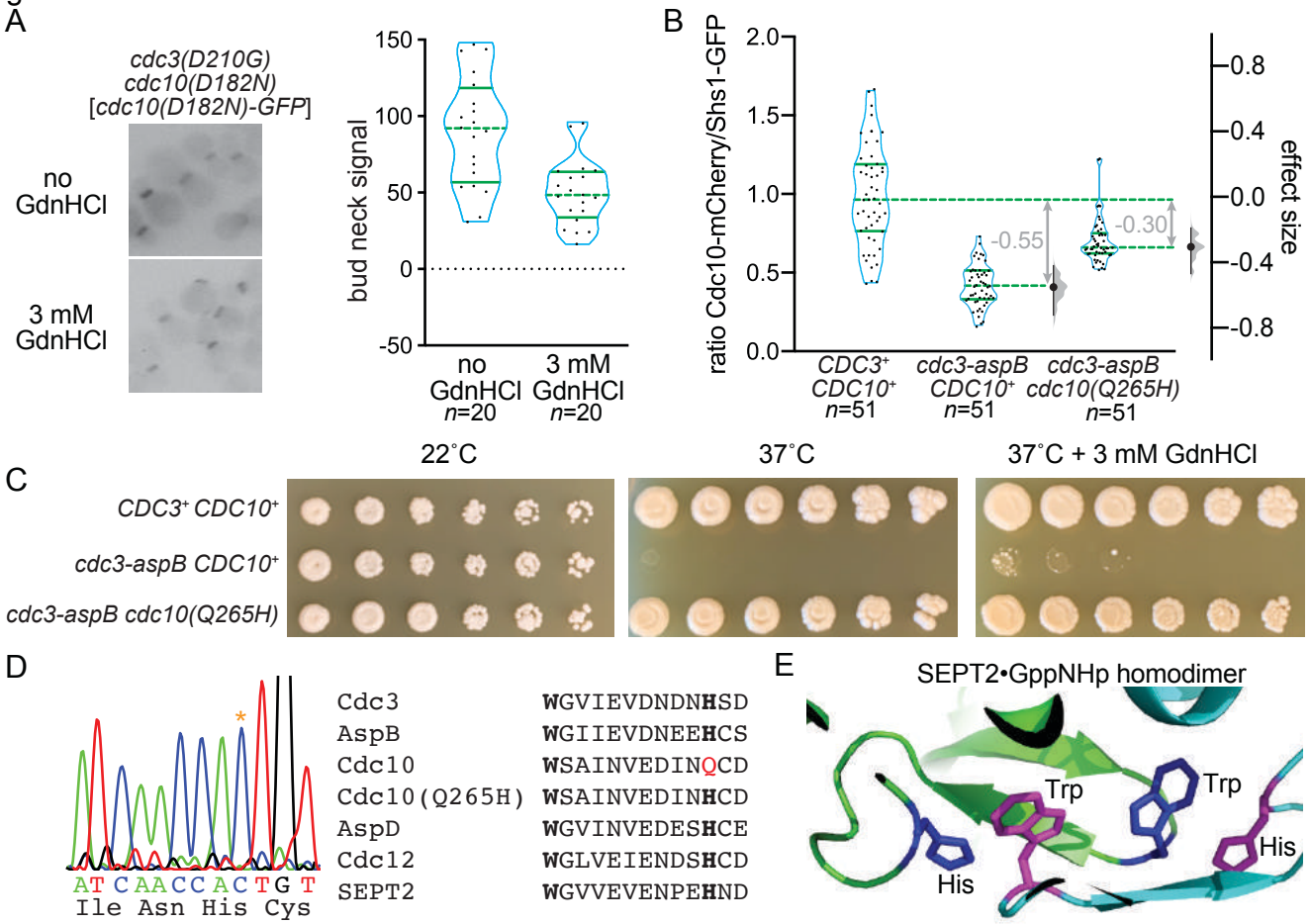
A
cdc3(D210G)
cdc10(D182N)
[cdc10(D182N)-GFP]
no GdnHCl
3 mM GdnHCl
bud neck signal
150
100
50
0
-50
no GdnHCl n=20
3 mM GdnHCl n=20
B
ratio Cdc10-mCherry/Shs1-GFP
2.0
1.5
1.0
0.5
0.0
effect size
0.8
0.4
0.0
-0.4
-0.8
-0.55
-0.30
CDC3+ CDC10+ n=51
cdc3-aspB CDC10+ n=51
cdc3-aspB cdc10(Q265H) n=51
C
22˚C
37˚C
37˚C + 3 mM GdnHCl
CDC3+ CDC10+
cdc3-aspB CDC10+
cdc3-aspB cdc10(Q265H)
D
*
AT C AACC AC T G T
Ile Asn His Cys
Cdc3 WGVIEVDNDNHSD
AspB WGIIEVDNEEHCS
Cdc10 WSAINVEDINQCD
Cdc10(Q265H) WSAINVEDINHCD
AspD WGVINVEDESHCE
Cdc12 WGLVEIENDSHCD
SEPT2 WGVVEVENPEHND
E
SEPT2•GppNHp homodimer
Trp
Trp
His
His

S1 Figure

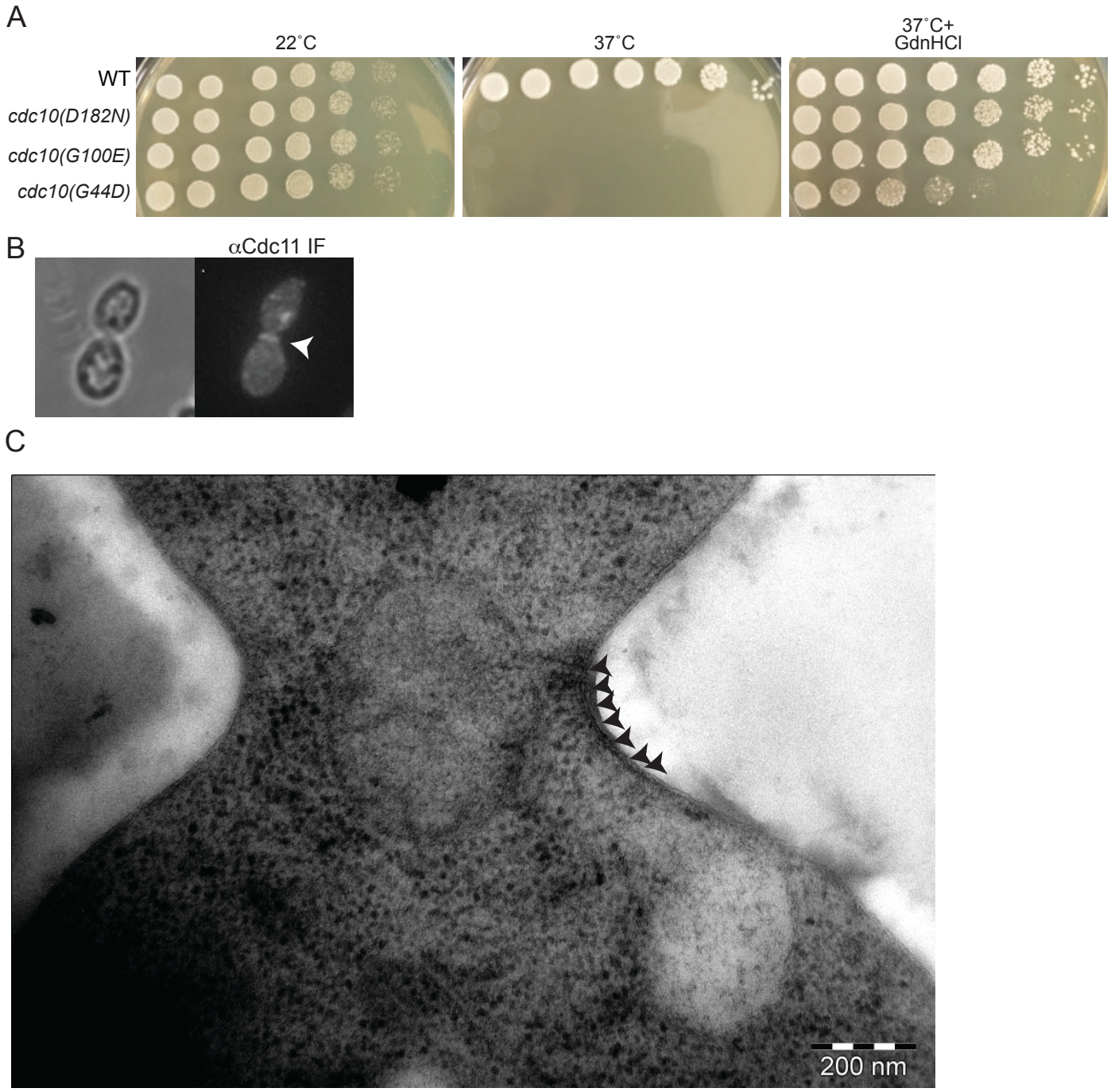
A
22˚C
37˚C
37˚C+
GdnHCl
WT
cdc10(D182N)
cdc10(G100E)
cdc10(G44D)
B
αCdc11 IF
C
200 nm

S2 Figure

```
                    (     α0      )            ---G1---
ScCdc3    95 QINGYVGFANLPKQWHRRSIKNGFSFNLLCVGPDGIGKTTLMKTLFNN  142
AgCdc3    89 KISGYVGFANLPKQWHRKSIRRGFNLNLLCVGAKGLGKSTLINTLFNK  136
KlCdc3    74 IINGYVGFANLPKQWHRKSIRRGFNLNLLCVGYKGLGKSTLINTLFNR  121
CaCdc3    23 VLNGYVGFANLPKQWHRKSIRRGFSLNIMAIGESGLGKATLINTLFNR  70
CcAspB    40 KLMGYVGFANLPNQVHRKSVRKGFQFTCMVVGESGLGKSTLVNTLFNT  87
UmCdc3    29 KLMGYVGFANLPNQVHRKSVRKGFNFTAMVVGESGLGKSTLINTLFNT  76
NcCdc3    60 KLTGYVGFANLPNQWHRKSVRKGFNFNVMVVGESGLGKSTLVNTLFNT  107
AnAspB     8 KLTGYVGFANLPNQWHRKSVRKGFNFNVMVVGESGLGKSTLVNTLFNT  55
MoSep3    46 KLTGYVGFANLPNQWHRKSVRKGFNFNVMVVGESGLGKSTLVNTLFNT  93
FgCdc3   165 KLTGYVGFANLPNQWHRKSVRKGFNFNVMVVGESGLGKSTLVNTLFNT  212
CnCdc3    60 KLSSWVGFSNLPNQVHRRSVRRGFQFVTMVVGESGLGKSTLINTLFET  107
SpSpn1    71 QLNGYVGFASLPNQWHRRCVRQGFNFNVLVLGESGSGKSTLVNTLLNR  118
HsSEPT2   12 ETPGYVGFANLPNQVHRKSVKKGFEFTLMVVGESGLGKSTLINSLFLT  60
HsSEPT9  256 VDFGYVGIDSILEQMRRKAMKQGFEFNIMVVGQSGLGKSTLINTLFKS  303

             -Sw I--                          -G4-   (      α4       )
ScCdc3    179 RHKVKIKSYESVIEE ... 278 KCNLIPVIAKSDILTDEEILSFKKTIMNQLIQSNIEL
AgCdc3    169 ENKVKIETVTTEIEE ... 267 KCNLIPVIAKSDILTDEEIEHFKWTIKKQLDDAKVHL
KlCdc3    160 ENKVKIETVSAEIEE ... 258 KCNLIPVIAKSDILTDEEIVTFKATIKKQLEQANVQL
CaCdc3     89 DVSVKIKSTQAEIEE ... 187 KVNLIPVIAKSDTLTDEEILEFKHRILADISHQGIKI
CcAspB    103 PKTVAIESIGADIEE ... 201 KVNLIPVIAKADTLTDEEVAEFKQRILADIAHHNIHI
UmCdc3     92 PKTVAIESISSDIEE ... 190 KVNLIPVIAKSDTLTDEEIVSFKQRILNDIAHHKIEI
NcCdc3    124 PKTVTIQSISADIEE ... 222 KVNLIPVIAKSDTLTDDEIAAFKARILADIKYHKVQI
AnAspB     72 PKTVSIQSISADIEE ... 170 KVNLIPVIAKADTLTDDEISMFKKRILADIQHHSIQI
MoSep3    110 PKTVTIQSISADIEE ... 208 KVNLIPVIAKSDTLTDEEIFAFKQRILADIKHHKVQI
FgCdc3    229 PKTVTIQSISADIEE ... 327 KVNLIPVIAKADTLTDEEIAAFKSRILADIKHHGIQI
CnCdc3    123 GKTVQIESISADIEE ... 221 KVNLIPIIAKADTMTDDEIIAFKQRILADIAHYGIQI
SpSpn1    137 EPTVMINSSAVEIVE ... 235 KVNIIPIIAKADTLTDDELNFTKEMILRDIQYHNIRI
HsSEPT2    76 ERTVQIEASTVEIEE ... 174 KVNIVPVIAKADTLTLKERERLKKRILDEIEEHNIKI
HsSEPT9   319 PKTIEIKSITHDIEE ... 272 VVNIVPVIAKADTLTLEERVHFKQRITADLLSNGIDV

              | C-terminal extension ->
ScCdc3    437  HEAKLAKLEIEMKTVF ... KEKLTKQLKALEDKK  516
AgCdc3    426  HEAKLAKLEAEMKAVF ... KEKLMKQLKALEEKK  502
KlCdc3    415  HEVKLAKLEAEMKAVF ... KDKLTSQLKALEEKK  491
CaCdc3    345  HEAKLAKMEAEMKSVF ... KDKLTKQIKLLEEKK  424
CcAspB    360  HEAKLAKMEAEMKMVF ... KDALEKQRAELEDKK  436
UmCdc3    349  HEARLRKMENEMKLVF ... RDALEKQRQELEEKR  425
NcCdc3    381  HEQKLAKMEAEMKMVF ... KEQLERQRLELEEKK  453
AnAspB    329  HEQKLAKMEAEMKMVF ... KEQLDRQRAELEEKK  400
MoSep3    367  HEQKLAKMEAEMKLVF ... KEQLDRQRAELEEKK  438
FgCdc3    486  HEQKLAKMEAEMKMVF ... KEQLDRQRLELEDKK  557
CnCdc3    380  HEAKLAKMEAEMKIVF ... KDALEKQKQELEDKR  456
SpSpn1    393  HEEKLMKMEAEMKTIF ... KAALEKQKADLIDHK  464
```

S3 Figure

```
Cdc3-AspB  1    MSLKEEQVSIKQDPEQEERQHDQFNDVQIKQESQDHDGVDSQYTNGTQNDDSERFEAAESDVKVEPGLGMGITSSQSEKG  80
AspB            --------------------------------------------------------------------------------
Cdc3       1    MSLKEEQVSIKQDPEQEERQHDQFNDVQIKQESQDHDGVDSQYTNGTQNDDSERFEAAESDVKVEPGLGMGITSSQSEKG  80

Cdc3-AspB  81   QVLPDQPEIKFIRRKLTGYVGFANLPNQWHRKSVRKGFNFNVMVVGESGLGKSTLVNTLFNTSL    YPPKERAGPSHD  156
AspB       1    -------MKNVVRRKLTGYVGFANLPNQWHRKSVRKGFNFNVMVVGESGLGKSTLVNTLFNTSL    YPPKERAGPSHD  69
Cdc3       81   QVLPDQPEIKFIRRQINGYVGFANLPKQWHRRSIKNGFSFNLLCVGPDGIGKTTLMKTLFNNDD[16]QEEEEGQGEGHE  172

Cdc3-AspB  157  IIPK   TVSIQSISADIEENGVRLRLTVVDTPGFGDFVNNDD-SWRPIVENIEQRYDAYLEAENKVNRTNIIDNRIHAC  232
AspB       70   IIPK   TVSIQSISADIEENGVRLRLTVVDTPGFGDFVNNDD-SWRPIVENIEQRYDAYLEAENKVNRTNIIDNRIHAC  145
Cdc3       173  NQSQ[4]KVKIKSYESVIEENGVKLNLNVIDTEGFGDFLNNDQKSWDPIIKEIDSRFDQYLDAENKINRHSINDKRIHAC  253

Cdc3-AspB  233  VYFIQPTGHSLKPLDIEVMRRLHTKVNLIPVIAKADTLTDDEISMFKKRILADIQHHSIQIFEGPRYELDDEETIAENQE  312
AspB       146  VYFIQPTGHSLKPLDIEVMRRLHTKVNLIPVIAKADTLTDDEISMFKKRILADIQHHSIQIFEGPRYELDDEETIAENQE  225
Cdc3       254  LYFIEPTGHYLKPLDLKFMQSVYEKCNLIPVIAKSDILTDEEILSFKKTIMNQLIQSNIELFKPPIYSNDDAENSHLSER  333

Cdc3-AspB  313  IMSKVPFAVIGSNDIVENYSGNQVRGRSYPWGVIEVDNDNHSDFNLLKNLLIKQFMEELKERTSKILYENYRSSKLAKLG  392
AspB       226  IMSKVPFAVVGANSEVATSDGRKVRGRSYPWGIIEVDNEEHCSFVKLRQMLIRTHMEELKEHTNNHLYENYRSDKLTQMG  305
Cdc3       334  LFSSLPYAVIGSNDIVENYSGNQVRGRSYPWGVIEVDNDNHSDFNLLKNLLIKQFMEELKERTSKILYENYRSSKLAKLG  413

Cdc3-AspB  393  IKQDNSVFKEFDPISKQLEEKTLHEAKLAKLEIEMKTVFQQKVSEKEKKLQKSETELFARHKEMKEKLTKQLKALEDKKK  472
AspB       306  VAQDPSVFKEVNPAVKQEEEDALHEQKLAKMEAEMKMVFQQKVAEKESKLKQSEDELYARHREMKEQLDRQRAELEEKKA  385
Cdc3       414  IKQDNSVFKEFDPISKQQEEKTLHEAKLAKLEIEMKTVFQQKVSEKEKKLQKSETELFARHKEMKEKLTKQLKALEDKKK  493

Cdc3-AspB  473  QLELSINSASPNVNHSPVPTKKKGF-LR*  500
AspB       386  RLE----SGRPLEEKG----KRKGFSLR*  405
Cdc3       494  QLELSINSASPNVNHSPVPTKKKGF-LR*  521
```

```
          ---G1---       -Sw I--      α4        )
ScCdc3    GPDGIGKTT ... RHKVKIK ... KKTIMNQLIQ
ScCdc12   GESGLGKTT ... RKTVEID ... KSRIRQVIEA
AnAspB    GESGLGKST ... PKTVSIQ ... KQRILADIKH
```

S4 Figure

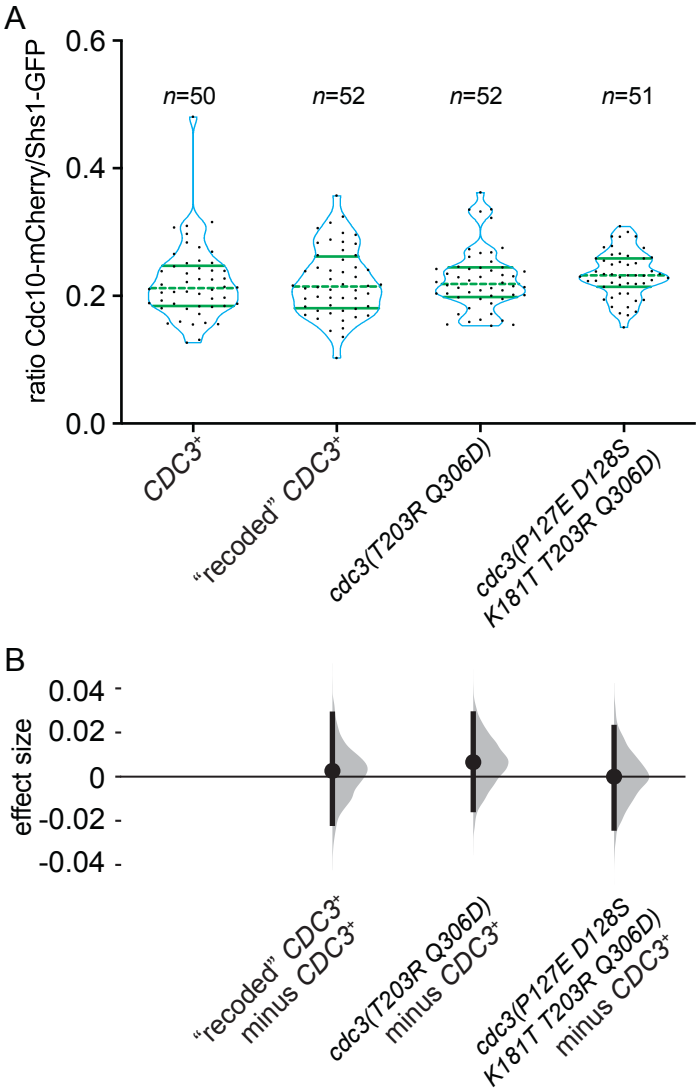
A
ratio Cdc10-mCherry/Shs1-GFP
0.6
0.4
0.2
0.0
n=50
n=52
n=52
n=51
CDC3+
"recoded" CDC3+
cdc3(T203R Q306D)
cdc3(P127E D128S K181T T203R Q306D)
B
effect size
0.04
0.02
0
-0.02
-0.04
"recoded" CDC3+ minus CDC3+
cdc3(T203R Q306D) minus CDC3+
cdc3(P127E D128S K181T T203R Q306D) minus CDC3+

S5 Figure

A

A. thaliana Toc34

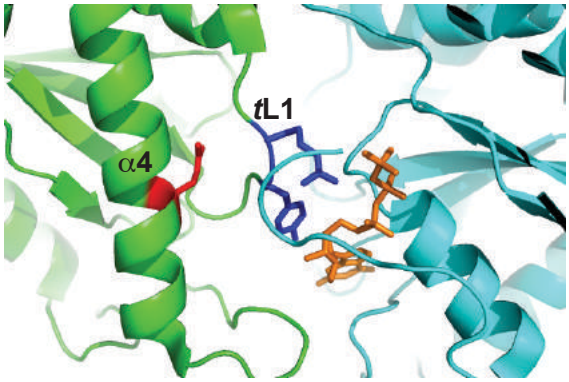

P. sativum Toc34

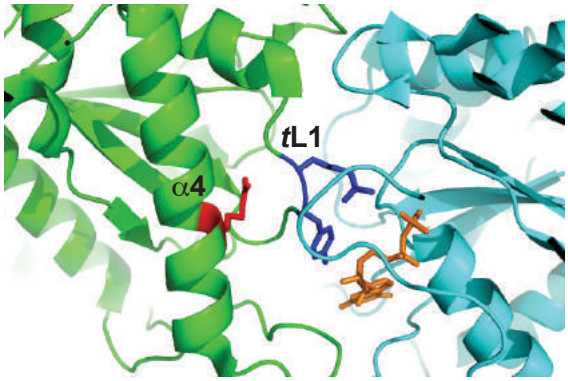

B

```
                        (          α4
At 160   LTHAQFSPPDGLNYNHFVSKRSNALL
Al 160   LTHAQFSPPDGLNYNSFVSRRSDALL
Cs 160   LTHAQFSPPDGLNYDLFVSRRSDALL
Bn 160   LSHAQFSPPDGLNYDLFVSRRSDALL
Nc 160   LTHAQFSPPDGLNYDLFVSRRSDALL
Br 160   LSHAQFSPPDGLNYDLFVSRRSDALL
Es 160   LSHAQFSPPDGLNYDLFVSRRSDALL
Vv 159   LTHAQLSPPDGLNYEDFFSKRSEALM
Eg 159   LTHAQLSPPDGLEYDLFFSKRSEALM
Ps 161   LTHAQFSPPDGLPYDEFFSKRSEALL
Nt 159   LSHAQLSPPDGLTYDEFTSQRSEALL
Zm 159   LTHAQLSPPDGIDYNDFFTRRSEALL
```

S6 Figure

```
Sc      AKSDILTDEEILSFKKTIMNQLIQSNIELFKP  317
Sp 95%  AKSDILTDEEILSFKKTIMNQLIQSNIELFKP  313
Sm 89%  AKSDILTDEEILNFKKAIMNQLIQSNIELFKP  313
Sa 87%  AKSDILTDEEILNFKKTIMNQLVQSDIKLFKP  312
Sb 86%  AKSDILTDEEILNFKKSIMGQLAQSNIELFKP  375
Su 86%  AKSDILTDEEILNFKKSIMGQLAQSNIELFKP  375
Sk 86%  AKSDILTDEEILNFKKAIMNQLIESNIKLFKP  313

Ca      AKSDTLTDEEILEFKHRILADISHQGIKIFKP  226
Cd 99%  AKSDTLTDEEILEFKHRILADISHQGIKIFKP  226
Cm 91%  AKSDTLTDEEILEFKHRILADITHQGIKIFQP  225
Cr 90%  AKSDTLTDEEILEFKHRILADITYQGIKIFKP  226
Ct 38%  AKSDTMSPVELDNFKSRIRDIIEAQDINIYTP  203
Cg 35%  SKADTLTAQELQLFKSRIRQVIEAQEIAIFTP  198
```

S7 Figure

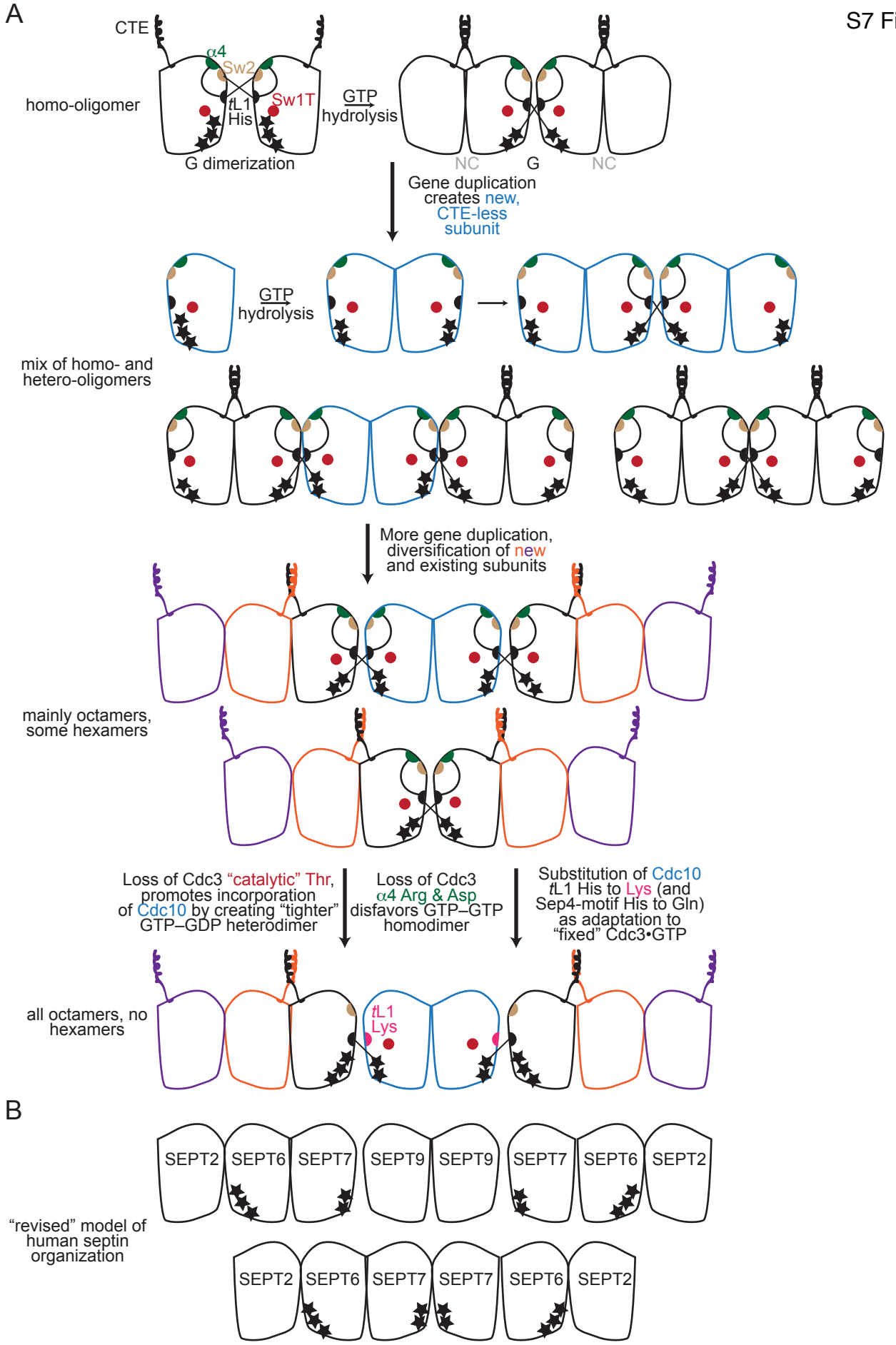
A
CTE
α4
Sw2
Sw1T
tL1
His
homo-oligomer
G dimerization
GTP
hydrolysis
NC
G
NC
Gene duplication
creates new,
CTE-less
subunit
GTP
hydrolysis
mix of homo- and
hetero-oligomers
More gene duplication,
diversification of new
and existing subunits
mainly octamers,
some hexamers
Loss of Cdc3 "catalytic" Thr,
promotes incorporation
of Cdc10 by creating "tighter"
GTP–GDP heterodimer
Loss of Cdc3
α4 Arg & Asp
disfavors GTP–GTP
homodimer
Substitution of Cdc10
tL1 His to Lys (and
Sep4-motif His to Gln)
as adaptation to
"fixed" Cdc3•GTP
all octamers, no
hexamers
tL1
Lys
B
SEPT2
SEPT6
SEPT7
SEPT9
SEPT9
SEPT7
SEPT6
SEPT2
"revised" model of
human septin
organization
SEPT2
SEPT6
SEPT7
SEPT7
SEPT6
SEPT2